Published June 20, 2011

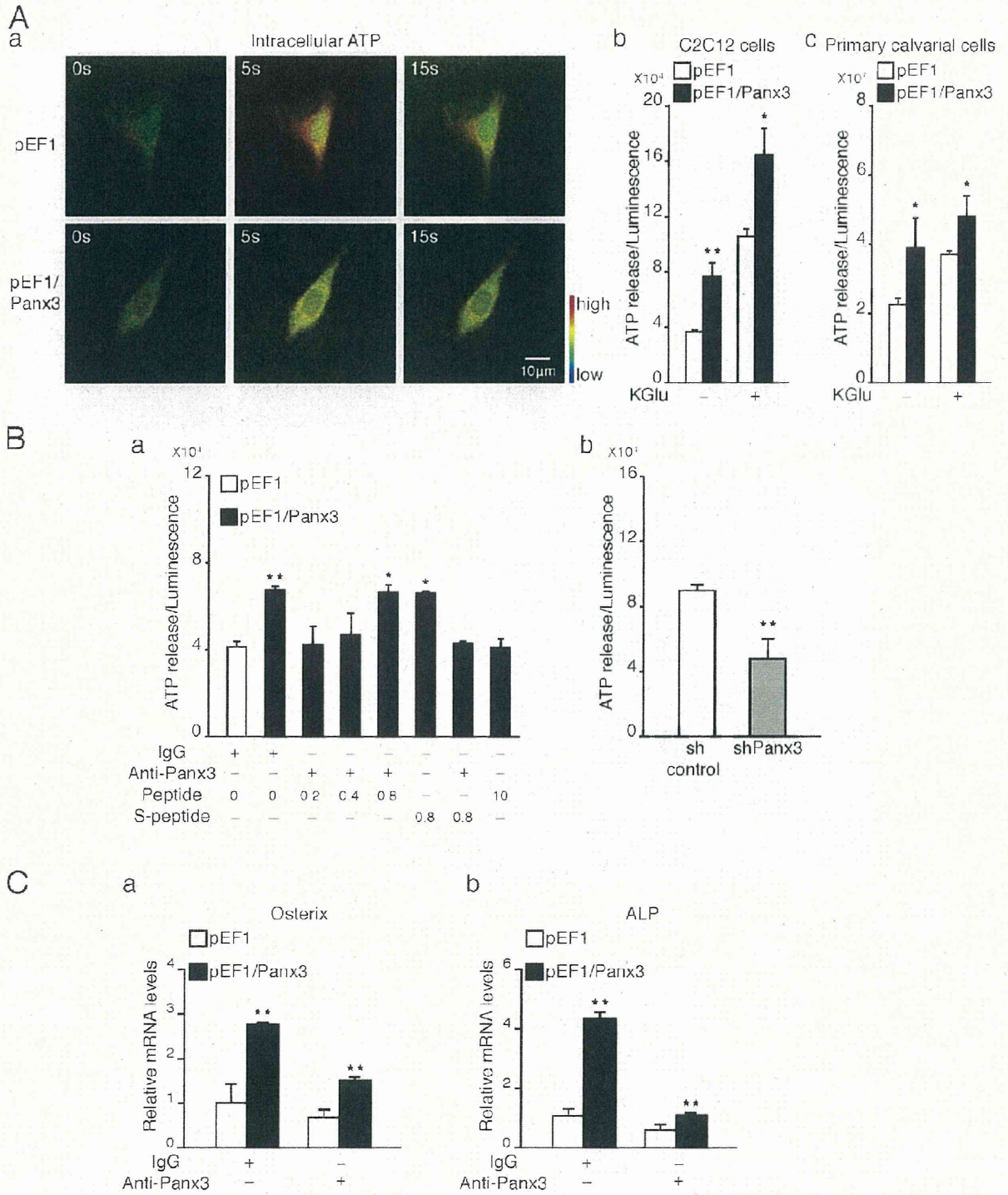

Figure 8. **Panx3 hemichannel releases intracellular ATP and promotes differentiation.** (A) Imaging of intracellular ATP levels in pEF1- or pEF1/Panx3-transfected C2C12 cells. Cells were incubated with the caged luciferin, and then exposed to a flash of UV light for photolysis to convert active luciferin. Fluorescence excitation images (red) caused by luciferin–ATP interactions at 5 s and 15 s after a UV flash were shown. Higher red fluorescence images were observed in control pEF1-transfected cells compared with Panx3-overexpressing cells, which indicates that Panx3 overexpression reduced intracellular ATP levels. (A, b and c) Measurement of ATP release. The transfected C2C12 cells or primary calvarial cells were treated with or without KGlu for 2 min, and then ATP released into the media was measured. (B) Inhibition of ATP release. The transfected cells were incubated with Panx3 antibody or Panx3 peptide for 30 min, and ATP release was measured. The Panx3 antibody (1.5 μg/ml) inhibited ATP release in pEF1/Panx3-transfected cells (a). This inhibition was blocked by various concentrations of the Panx3 peptide. The Panx3 peptide also inhibited the ATP release (a). Control sh- or shPanx3-transfected cells were cultured with BMP2 for 2 d, and ATP release was measured. ATP release was reduced in shPanx3-transfected cells compared with control sh-transfected cells (b). (C) Inhibition of osterix (a) and ALP (b) expression by the anti-Panx3 antibody. *, $P < 0.05$; **, $P < 0.01$. Error bars represent the mean ± SD; $n = 3$.

Published June 20, 2011

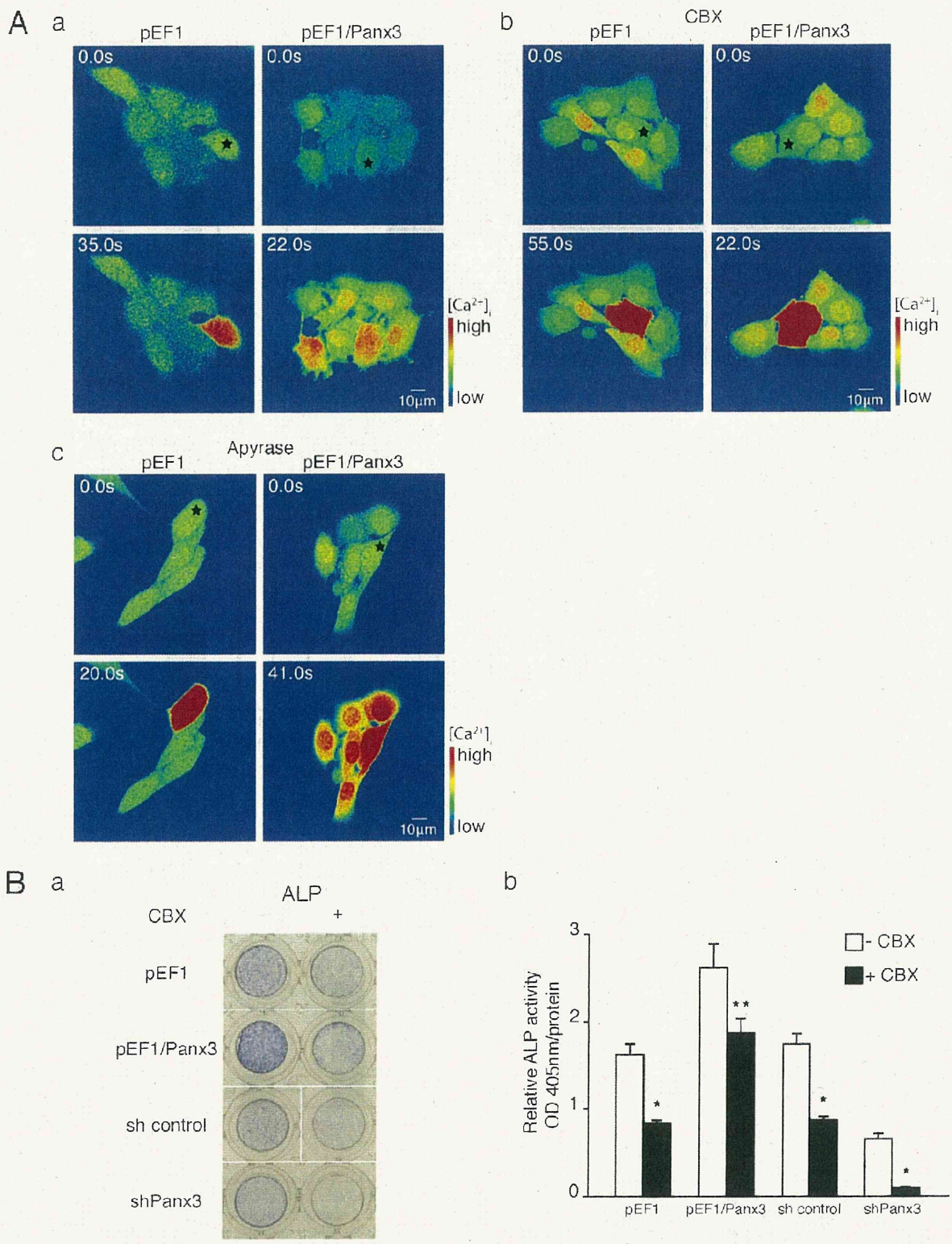

Figure 9. **Panx3 functions as a gap junction.** (A) Real-time imaging of Ca^{2+} wave propagation. The Ca^{2+} wave was measured in cells loaded with Fluo-4 and NP-EGTA (caged Ca^{2+}) by starting photolysis of NP-EGTA in a single cell using a flash of UV light. (a) pEF1/Panx3-transfected cells, but not pEF1-transfected cells, propagated Ca^{2+} waves to neighboring cells. (b) Inhibition of the Ca^{2+} wave propagation by CBX (gap junction inhibitor). (c) Apyrase, ATP receptor antagonist, did not inhibit Ca^{2+} propagation in pEF1/Panx3-transfected cells. (B) CBX inhibited C2C12 cell differentiation. (a) ALP staining. (b) Quantitative data from the ALP staining. CBX inhibited osteoblast differentiation in pEF1/Panx3-transfected cells (a and b). *, $P < 0.05$; **, $P < 0.01$. Error bars represent the mean ± SD; $n = 3$.

Published June 20, 2011

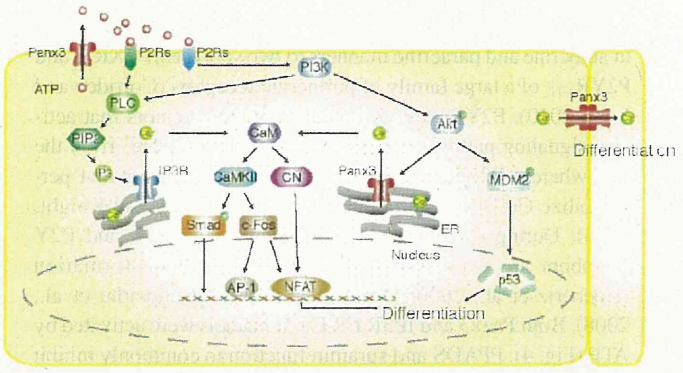

Figure 10. **Panx3 pathways in osteoblast differentiation.** The Panx3 hemichannel releases intracellular ATP. The released ATP binds to purinoreceptors (P2Rs) in its own cell and/or neighboring cells, and activates the PI3K–Akt pathway. Akt then activates the Panx3 ER Ca^{2+} channel to increase $[Ca^{2+}]_i$ levels, which leads to activation of the CaM–CaMKII pathway. The ATP also activates the PLC–PIP2–IP3R ER Ca^{2+} channel pathway, which is distinct from that of the Panx3 ER Ca^{2+} channel. The Akt activation also phosphorylates MDM2, which induces degradation of p53, an inhibitor for osteogenic differentiation, and promotes differentiation. CaM also activates CN, which dephosphorylates inactive phosphorylated NFAT in cytosol. Dephosphorylated NFATc1 enters the nucleus and binds to the promoter regions of differentiation genes such as osterix and ALP. Activated CaMKII also increases c-fos and NFAT expression, and activation of Ap-1 and Smad1/5. Panx3 gap junction activity promotes Ca^{2+} wave propagation between adjacent cells for differentiation.

single cell within a cell network was subjected to two-photon photolysis. The uncaged Ca^{2+} fluctuations were analyzed by live-cell fluorescence confocal microscopy (Fig. 9 A, a; and Videos 5 and 6). We also observed similar Ca^{2+} wave propagation in Panx3-overexpressing calvarial cells (unpublished data). In Panx3-overexpressing cells, Ca^{2+} waves were propagated into neighboring cells (red in high Ca^{2+}), whereas in control cells lacking Panx3, the Ca^{2+} fluctuations were restricted to the single uncaged cell. This Ca^{2+} wave propagation was inhibited by the gap junction inhibitor carbenoxolone (CBX; Fig. 9 A, b; and Videos 7 and 8). Because CBX may disrupt the cell membrane and affect activation of P2 receptors, thereby inhibiting the Ca^{2+} wave, apyrase (an ATP receptor antagonist) was added to the Ca^{2+} wave assay at a concentration, which inhibited Panx3-mediated activation of Akt signaling (Fig. S3). We found that apyrase did not inhibit the Ca^{2+} wave, which suggests that Panx3 gap junction mediates Ca^{2+} wave propagation (Fig. 9 A, c; and Videos 9 and 10). To test the effect of Panx3-mediated gap junction activity on C2C12 cell differentiation, Panx3-overexpressing and control cells were induced to differentiate by BMP2 treatment in the presence of CBX, and ALP activity was measured (Fig. 9 B). Panx3 overexpression promoted ALP activity, as shown in Fig. 2, but CBX inhibited this ALP activation. Similarly, Panx3 shRNA inhibited ALP induction, as shown in Fig. 2, and CBX further inhibited ALP activity. These results indicated that Panx3 can function as a gap junction and propagate Ca^{2+} waves from cell to cell, and that this activity also promotes osteoblast differentiation.

Discussion

In our present study, we demonstrated for the first time that Panx3 regulates osteoblast differentiation through its multiple functions as a hemichannel, an ER Ca^{2+} channel, and a gap junction, as illustrated in Fig. 10. All three Panx3 activities are associated with and involved in osteoblast differentiation. We showed that Panx3 is induced during osteogenic differentiation and is localized in the plasma membrane, and that it functions as the hemichannel that releases ATP into the extracellular space. The ATP released from the cells binds to purinergic receptors (P2Rs) in the plasma membrane in an autocrine and paracrine manner, and thereby activates P2R–PI3K–Akt signaling for the Panx3 channel and P2R–PLC–PIP2–IP3 for the IP3R channel. Akt-mediated Panx3 ER Ca^{2+} channel activation induces Ca^{2+} release from the ER into the cytosol, which subsequently activates CaM signaling pathways, including CaMKII–Smad, CaMKII–c-Fos, and CN–NFATc. The Akt activation also increases p53 degradation through activation of MDM2. The activation of these pathways promotes differentiation. In addition, the increased $[Ca^{2+}]_i$ level that originated in cells because of the hemichannel in turn propagates its wave into surrounding cells through a Panx3 gap junction, subsequently promoting Ca^{2+} signaling among cell populations for differentiation. Because blocking of the Panx3 hemichannel inhibits osteoblast differentiation, this hemichannel activation may be the first step in Panx3-mediated differentiation processes.

Ca^{2+} is one of the most important second messengers and regulates many cellular processes (Berridge et al., 2000b), and the CaM pathway is critical for osteoblast differentiation (Zayzafoon, 2006). However, the mechanism for controlling $[Ca^{2+}]_i$ during osteoblast differentiation is not yet clear. We found that Panx3 functions as a Ca^{2+} channel in the ER, through which it regulates $[Ca^{2+}]_i$. C2C12 and calvarial cells express IP3Rs. Both Panx3 and IP3Rs function as ER Ca^{2+} channels; however, their activation mechanisms are different. We found that the Panx3 ER Ca^{2+} channel was activated through Akt signaling (Fig. 7 A), distinct from IP3-mediated activation of ubiquitous IP3R ER Ca^{2+} channels (Mikoshiba, 2007). In addition, siRNA for IP3R3 and 2-APB, which is an inhibitor of IP3R-mediated Ca^{2+} release, inhibited IP3R ER Ca^{2+} channel activity, but did not inhibit the Panx3 channel (Fig. 5 A). The role of IP3Rs in osteogenic differentiation is also not yet clear. The inhibition of endogenous Panx3 by shRNA resulted in substantial inhibition of osteogenic differentiation in C2C12 cells, despite IP3R expression, whereas the inhibition of IP3Rs by siRNA and 2-APB showed limited inhibition of C2C12 cell differentiation (unpublished data). In addition, mice lacking either IP3R2 or IP3R3 were viable and had no obvious abnormalities. Mice lacking both IP3R2 and IP3R3 were born with a normal appearance but began losing body weight after weaning because of defects in exocrine secretion (Futatsugi et al., 2005). Both receptors may function as ER Ca^{2+} channels with distinct activation mechanisms during osteogenic differentiation. Because the Panx3 hemichannel likely triggers activation of these Panx3 and IP3R ER Ca^{2+} channels, Panx3 may play a major role upstream of IP3Rs in osteogenic differentiation.

Published June 20, 2011

Extracellular ATP modulates cellular functions by binding in autocrine and paracrine manners to two subtypes, $P2XR_{1-7}$ and $P2YR_{1-12}$, of a large family of purinergic receptors (Corriden and Insel, 2010). P2YRs are G protein–coupled receptors that activate signaling pathways responsible for releasing Ca^{2+} from the ER, whereas P2XRs are nonselective cation channels that permeabilize Ca^{2+}, Na^{+}, and other cations (Burnstock and Knight, 2004). During osteoblast differentiation, many P2X and P2Y members are expressed and implicated in bone formation (Hoebertz et al., 2000; Orriss et al., 2006; Panupinthu et al., 2008). Both Panx3 and IP3R ER Ca^{2+} channels were activated by ATP (Fig. 4). PPADS and suramin function to commonly inhibit some P2Ys and P2XRs (e.g., P2X1, P2X3, and P2Y6); however, they also inhibit specifically (e.g., PPADS for P2Y1 and P2Y4; suramin for P2X2, P2X5, and P2Y2; P2 receptors; Burnstock, 2007). Panx3 ER Ca^{2+} channels, but not IP3R ER Ca^{2+} channels, were inhibited by PPADS (Boyer et al., 1994; Ziganshin et al., 1994), whereas suramin inhibited both channels (Fig. 5 B). These results suggest that the Panx3 and IP3R ER Ca^{2+} channels may be regulated through different purinergic receptors. The ATP-induced $[Ca^{2+}]_i$ experiments were performed in cell culture without external Ca^{2+} in the medium to measure $[Ca^{2+}]_i$ released from the ER. However, in vivo, external Ca^{2+} may also contribute to an increase in $[Ca^{2+}]_i$ through the ATP-P2X cation channels. Indeed, P2X7 knockout mice displayed reduced periosteal bone formation and response to mechanical loading (Ke et al., 2003; Li et al., 2005).

Panx3 expression increased phosphorylation of Akt (Fig. 6 A). Akt signaling is required for osteoblast differentiation, bone formation, and prevention of osteoblast apoptosis (Kawamura et al., 2007; Mukherjee and Rotwein, 2009). One of the Akt target pathways is the MDM2/p53 signaling pathway (Lengner et al., 2006; Wang et al., 2006). Panx3 expression promoted phosphorylation of MDM2 and enhanced the degradation of the p53 protein (Fig. 6 A). These results indicate that Panx3-promoted osteogenic differentiation occurs in part due to reduction of the p53 level through enhancement of the Akt–MDM2–p53 pathway (Fig. 10). We found that Panx3 also stimulated phosphorylation of Smad1/5 (Fig. 5 C). Previous studies have shown that CaM–CaMKII activates Smad1/5 (Scherer and Graff, 2000), and therefore, Panx3 ER Ca^{2+} channel/CaM–CaMKII signaling activates Smad1/5. The anti-Panx3 antibody and PPADS inhibited the Panx3-promoted Smad1/5 activation, which suggests that the Panx3 hemichannel and P2Rs are involved in these processes.

Panx1 and Panx2 were expressed in C2C12 and primary calvarial cells at a very low level and were not induced at all during osteogenic differentiation of these cells (unpublished data). Therefore, Panx3 is the major pannexin protein expressed during osteoblast differentiation. Among the connexin gap junction proteins, Cx43 is the most highly expressed in osteoblasts (Civitelli et al., 1993; Su et al., 1997; Gramsch et al., 2001; Jiang et al., 2007), and is implicated in osteoblast differentiation and mineralization (Lecanda et al., 2000; Stains and Civitelli, 2005; Chung et al., 2006; Inose et al., 2009). Cx43 knockout mice showed cranial abnormalities and delayed ossification, whereas axial and appendicular elements were normal at birth (Lecanda et al., 2000). Mice with conditional Cx43 deletion in osteoblasts displayed a normal appearance at birth but developed a low bone density osteopenia phenotype with age (Chung et al., 2006). Panx3 overexpression in differentiated C2C12 cells promoted Cx43 expression, whereas suppression of endogenous Panx3 by Panx3 shRNA inhibited Cx43 expression (unpublished data). These results suggest that Panx3 and Cx43 may play distinct roles in osteogenic differentiation.

In summary, we have provided evidence that Panx3 acts as a multifunctional protein that promotes osteoblast differentiation by regulating Akt and Ca^{2+} signaling through its hemichannel, ER channel, and gap junction activities.

Materials and methods

Reagents

Rabbit anti-Panx3 antibody, inhibitory Panx3 and scrambled peptides, Panx3 expression vector (pEF1/Panx3) and control vector (pEF1), shRNA vector for Panx3 (shPanx3), and control vector (sh control) have been described previously (Iwamoto et al., 2010). In brief, the pEF1/Panx3 vector was constructed by cloning the coding sequence of mouse Panx3 cDNA into the pEF1/V5-His vector (Invitrogen). The shPanx3 vector containing the 3′ untranslated region of Panx3 (5′-GGCAGGGTAGAACAATTTA-3′) in a pSM2 vector was obtained from Thermo Fisher Scientific. A rabbit polyclonal antibody to a peptide (amino acid residues HHTQDKAGQYKVK-SLWPH) from the mouse Panx3 protein was generated and purified with a peptide affinity column. This Panx3 peptide was also used for inhibition experiments. A peptide with a scrambled sequence (WHTKYQVGLDPQH-KASHK) of the Panx3 peptide was used as a control. Control adenovirus (Ad-Cont) and Panx3 expression adenovirus (Ad-Panx3) were prepared and purified by Welgen, Inc. Akt CA and Akt DN vectors were obtained from Addgene. Antibodies for P-Rb, CaM, CaMKII, P-CaMKII, CN, p53, Akt, p-Akt, Smad1, and P-Smad1/5 were obtained from Cell Signaling Technology; Rb, P-NFATc1, and MDM2 were from Santa Cruz Biotechnology, Inc.; NFATc1 was from BD; α-tubulin from Sigma-Aldrich; Ocn from Biomedical Technology; and calnexin from Thermo Fisher Scientific. 2-APB, U-73122, thapsigargin, PPADS, suramin, CBX, and apyrase were obtained from Sigma-Aldrich; Akt inhibitor was from EMD; LY294002 and Fura-2AM were from Invitrogen; BMP2 was from Humanzyme; and iQ SYBR Green Supermix was from Bio-Rad Laboratories. HRP-conjugated goat anti–mouse and goat anti–rabbit IgG were obtained from United States Biological.

Cell culture

Mouse C2C12 cells were grown in DME (Invitrogen) containing 10% FBS (HyClone) at 37°C under 5% CO_2. For osteoblast differentiation, cells (~90% confluence) were transiently or stably transfected with pEF1/Panx3, control vector, Panx3 shRNA, or sh control vector and cultured in the presence of 300 ng/ml BMP2 (Humanzyme) and 2% FBS. The media were replaced every 3 d. Primary calvarial cells were prepared from calvaria of newborn mice as described previously (Matsunobu et al., 2009). Calvaria were digested six times for 10 min with 0.1% collagenase type 1 (Worthington Biochemical Corp.) and 0.2% dispase II (Roche) in PBS. The last two fractions were centrifuged at 1,500 rpm for 5 min, resuspended in culture medium consisting of α-minimum essential medium (Invitrogen) with 10% FBS (HyClone), 100 U/ml of penicillin, and 100 µg/ml of streptomycin. Primary calvarial cells were transiently transfected with Nucleofector (Lonza). For the differentiation assay, primary calvarial cells were induced by the addition of 50 µg/ml ascorbic acid (Sigma-Aldrich) and 5 mM β-glycerophosphate (Sigma-Aldrich).

Immunostaining

Growth plates of newborn mice were fixed overnight in 4% paraformaldehyde and dehydrated before they were embedded in paraffin. After deparaffinization and rehydration, sections were digested with pepsin (Biocare Medical), blocked by Rodent block (Biocare Medical), and then reacted with primary antibodies for 2 h at room temperature. In cell culture, C2C12 cells were blocked by Power block (Biocare Medical) and reacted with primary antibodies under the same condition as described in the Cell culture section. Primary antibodies were detected by Alexa Fluor 488 (Invitrogen)- or Cy-3 (Jackson ImmunoResearch Laboratories)-conjugated

Published June 20, 2011

secondary antibodies. Nuclear staining was performed with Hoechst dye (Sigma-Aldrich). Analysis was performed on an inverted confocal microscope (LSM 510) and a fluorescence microscope (Axiovert 200; both from Carl Zeiss). Colocalization was analyzed by MetaMorph (Molecular Devices).

RT-PCR

Total RNA was extracted using the Nuclear Extraction System Quick-Gene-810 and HC kit S (Fujifilm). Total RNA (1 µg) was used for reverse transcription to generate cDNA, which was used as a template for PCRs with gene-specific primers (Table S1), as described previously (Iwamoto et al., 2010). The cDNA was amplified with an initial denaturation at 95°C for 3 min; then 95°C for 30 s, 60°C for 30 s, and 72°C for 30 s for 30 cycles; and then amplified with a final elongation step at 72°C for 5 min before being separated on agarose gels. Real-time PCR amplification was performed with iQ SYBR Green Supermix (Bio-Rad Laboratories) and a Chromo4 thermocycler (Bio-Rad Laboratories). Real-time PCR was performed for 40 cycles at 95°C for 1 min, 60°C for 1 min, and 72°C for 1 min. Gene expression was normalized to the housekeeping gene Hprt.

ATP flux

ATP flux was determined by luminometry, as described previously (Iwamoto et al., 2010). To open the pannexin channels, the cells were depolarized by incubation in KGlu solution (140 mM KGlu, 10 mM KCl, and 5.0 mM TES, pH 7.5) for 10 min. The supernatant was collected and assayed with luciferase/luciferin (Promega). The luminescence was measured using a multimode plate reader, Mithras LB 940 (Berthold). For inhibition by the Panx3-antibody, the cells were incubated with 1.5 ng/ml affinity-purified antibody or control IgG for 30 min before assay.

Western blot analysis

The cells were washed three times with PBS containing 1 mM sodium vanadate (Na_3VO_4), then solubilized in 100 µl of lysis buffer (10 mM Tris-HCl, pH 7.4, 150 mM NaCl, 10 mM $MgCl_2$, 0.5% Nonidet P-40, 1 mM phenylmethylsulfonyl fluoride, and 20 U/ml aprotinin). Lysed cells were centrifuged at 14,000 rpm for 30 min, and the protein concentration of each sample was measured with Micro-BCA Assay Reagent (Thermo Fisher Scientific). A 10 µg sample of each protein was electrophoresed in 4–12% SDS-polyacrylamide gel (Invitrogen) and transferred onto a polyvinylidene difluoride membrane using iBlot (Invitrogen). The membranes were immunoblotted with antibodies using standard protocols.

ALP assay

C2C12 cells and primary calvarial cells were plated into 12- or 96-well culture plates and grown to 100% confluence. The cells were then induced to differentiate into osteoblasts by addition of 300 ng/ml BMP2. ALP activity was measured in cell layers using a *p*-nitrophenyl phosphate substrate and an incubation temperature of 37°C, or was determined by the tartrate-resistant acid phosphatase (TRACP) & ALP double-stain kit (Takara Bio Inc.). The protein concentration was determined by the BCA protein assay method (Thermo Fisher Scientific).

Alizarin red S staining

C2C12 cells were fixed with 60% isopropanol and stained with 1% (wt/vol) Alizarin red S (Sigma-Aldrich). Calcium deposition was quantified as previously described (Mukherjee and Rotwein, 2009). In brief, the cultures were extracted from the Alizarin red S stain with 10% cetylpyridinium chloride (Sigma-Aldrich), and the OD was measured at 550 nm.

Ex vivo metatarsal bone culture

Metatarsal bones were isolated from newborn C57BL/6 mice and were cultured in DME containing 0.5% bovine serum albumin, 50 µg/ml ascorbic acid (Sigma-Aldrich), and 1 mM β-glycerol phosphate (Sigma-Aldrich) at 37°C in a humidified atmosphere of 5% CO_2, as described previously (Mukherjee and Rotwein, 2009). One day after starting the culture, the metatarsal bones were infected with Ad-Cont or Ad-Panx3 (1×10^9 PFU/ml) for 3 d. For the peptide inhibition assay, Panx3 antigen peptide or a scramble peptide (100 µg/ml) was added to the metatarsal cultures and incubated for 3 d. Live images were captured with a camera (Infinity2; Lumenera) attached to a microscope (Axiovert 25; Karl Zeiss). Images were analyzed and adjusted using MetaMorph (Molecular Devices) and National Institutes of Health ImageJ software. Metatarsals were fixed in 4% paraformaldehyde overnight at 4°C and stored in 70% ethanol. Bones were embedded in paraffin blocks and sectioned. Sections were stained with hematoxylin and eosin. Images were captured with microscope camera (AxioCam; Carl Zeiss) attached to a microscope (Axiovert 135; Carl Zeiss).

$[Ca^{2+}]_i$ measurements

C2C12 cells were grown in a 96-well plate for 3 d and then loaded with 5 µM Fura-2AM (Invitrogen) prepared in HBSS for 45 min at 37°C in 5% CO_2. After 3 d of transfection, transiently transfected primary calvarial cells were loaded at the same condition as the C2C12 cells. The Ca^{2+} transients were recorded as the 340/380 nm ratio (R) of the resulting 510-nm emissions using a plate reader (Mithras LB 940; Berthold Technologies). For the stimulation, 200 µM of ATP was automatically injected into cells by the Mithras 940. For inhibition experiments, cells were incubated for 30 min before analysis with one of the following inhibitors: 5 M U-73122 for IP3 synthesis inhibition, 100 µM 2-APB for blocking IP3R, 0.5 µM thapsigargin for SERCA ER Ca^{2+} pump inactivation, 100 µM PPADS, and 300 µM suramin for P2Rs inhibition; 5 µM Akt inhibitor; and 100 µM LY294002 for PI3K inhibition. The C2C12 cells that had been stably transfected with either pEF1/Panx3 or control vector were then transiently transfected with siIP3R-3 (Thermo Fisher Scientific). After 3 d of transfection, $[Ca^{2+}]_i$ was measured. The $[Ca^{2+}]_i$ levels were calculated as described previously (Grynkiewicz et al., 1985) using the equation $[Ca^{2+}]_i = K_d (R - R_{min})/(R_{max} - R)(F^{380}{}_{max}/F^{380}{}_{min})$, where R_{min} is the ratio at zero Ca^{2+}, R_{max} is the ratio when Fura-2 is completely saturated with Ca^{2+}, $F^{380}{}_{min}$ is the fluorescence at 380 nm for zero Ca^{2+}, and $F^{380}{}_{max}$ is the fluorescence at saturating Ca^{2+} and K_d = 224 nM.

Imaging of single-cell intracellular ATP concentrations and Ca^{2+} wave propagation

For the imaging of single-cell intracellular ATP levels, cells attached to glass-bottomed dishes (MatTek Corporation) were loaded with 25 µM of caged D-luciferin AM (Invitrogen) in HBSS containing 10 mM Hepes for 20 min at room temperature, followed by washing. The cells were then incubated with KGlu solution for 10 min. For Ca^{2+} wave propagation, cells seeded in a glass bottom dish were incubated in HBSS containing 4 µM of the Ca^{2+} indicator Fluo-4 AM, 10 µM pluronic F-127 (Invitrogen), 0.1% OxyFluor (Oxyrase), and 2.5 µM caged reagent NP-EGTA AM (Invitrogen) for 30 min at room temperature, followed by washing and incubation with Ca^{2+}-free HBSS. Both luciferin AM and Fluo-AM were imaged using a microscope (LSM 510 NLO META) equipped with A-Plan-Apochromat 63× (1.4 NA) objective lenses (all from Carl Zeiss). A 488 nm argon laser line was used for excitation. Cells were imaged every 1 s for ~1 min after the uncaging step. D-Luciferin AM and NP-EGTA AM were uncaged using a two-photon laser set at 730 nm. A nucleus-sized region of interest was used for uncaging within single cells using the Zen software's bleach function (Carl Zeiss). To block the gap junction channels, cells were incubated with 25 µM CBX. To inhibit ATP receptors, cells were incubated with 20 U apyrase.

Focal microscopy images were obtained using a two-photon confocal microscope. 488 nm argon, 543 nm HeNe1, and 633 nm HeNe2 lasers were used to excite Cy2, Cy3, and Cy5 fluorophores, respectively. The pinholes for each laser line were aligned for optimal confocality. For DAPI illumination, the two-photon laser was tuned to 730 nm and used at ~3–8% power.

Data analysis

Each experiment was repeated several times. The data were analyzed by Prism 5 software. Statistical differences between two groups of data were analyzed with a Student's *t* test. A one-way ANOVA was used for the quantification of Alizarin red S staining. $P < 0.05$ was considered statistically significant.

Online supplemental material

Fig. S1 shows Panx3 expression levels in the pEF1/Panx3- and shPanx3-transfected C2C12 cells, and the protein expression levels for Panx3, IP3R3, and RyR3 in undifferentiated and differentiated C2C12 cells. Fig. S2 shows the effects of Panx3 expression or shPanx3 inhibition on calvarial cell differentiation and an increase in $[Ca^{2+}]$ levels during differentiation of calvarial cells. Fig. S3 shows the inhibition of Akt activation by apyrase in C2C12 cells transfected with pEF1/Panx3. Videos 1–4 show imaging of ex vivo metatarsal growth by infection with Panx3 adenovirus (AdPanx3) or treatment with the inhibitory Panx3 peptide. Videos 5–8 show imaging of the Ca^{2+} wave propagation in the pEF1/Panx3 transfected C2C12 cells with and without CBX, and Videos 9 and 10 show no inhibitory effects of apyrase on the Ca^{2+} wave propagation. Table S1 shows the primers used for semi-quantitative and quantitative RT-PCR. Online supplemental material is available at http://www.jcb.org/cgi/content/full/jcb.201101050/DC1.

We thank Patricia Forcinito, Tomoya Matsunobu, Akira Futatsugi, and Indu Ambudkar for their suggestions.

This work was supported by the Intramural Program of the National Institute of Dental and Craniofacial Research, National Institutes of Health (to Y. Yamada), and grant-in-aids (20791583 to T. Iwamoto) and (20679006 to S. Fukumoto) from the Ministry of Education, Science, and Culture of Japan. M. Ishikawa was supported in part by a Fellowship from the Japan Society for the Promotion of Science.

Submitted: 12 January 2011
Accepted: 25 May 2011

References

Baranova, A., D. Ivanov, N. Petrash, A. Pestova, M. Skoblov, I. Kelmanson, D. Shagin, S. Nazarenko, E. Geraymovych, O. Litvin, et al. 2004. The mammalian pannexin family is homologous to the invertebrate innexin gap junction proteins. *Genomics*. 83:706–716. doi:10.1016/j.ygeno.2003.09.025

Barbe, M.T., H. Monyer, and R. Bruzzone. 2006. Cell-cell communication beyond connexins: the pannexin channels. *Physiology (Bethesda)*. 21:103–114.

Beals, C.R., N.A. Clipstone, S.N. Ho, and G.R. Crabtree. 1997. Nuclear localization of NF-ATc by a calcineurin-dependent, cyclosporin-sensitive intramolecular interaction. *Genes Dev.* 11:824–834. doi:10.1101/gad.11.7.824

Bennett, M.V., and V.K. Verselis. 1992. Biophysics of gap junctions. *Semin. Cell Biol.* 3:29–47. doi:10.1016/S1043-4682(10)80006-6

Berridge, M.J., P. Lipp, and M.D. Bootman. 2000a. Signal transduction. The calcium entry pas de deux. *Science*. 287:1604–1605. doi:10.1126/science.287.5458.1604

Berridge, M.J., P. Lipp, and M.D. Bootman. 2000b. The versatility and universality of calcium signalling. *Nat. Rev. Mol. Cell Biol.* 1:11–21. doi:10.1038/35036035

Biswas, G., O.A. Adebanjo, B.D. Freedman, H.K. Anandatheerthavarada, C. Vijayasarathy, M. Zaidi, M. Kotlikoff, and N.G. Avadhani. 1999. Retrograde Ca2+ signaling in C2C12 skeletal myocytes in response to mitochondrial genetic and metabolic stress: a novel mode of inter-organelle crosstalk. *EMBO J.* 18:522–533. doi:10.1093/emboj/18.3.522

Bleasdale, J.E., N.R. Thakur, R.S. Gremban, G.L. Bundy, F.A. Fitzpatrick, R.J. Smith, and S. Bunting. 1990. Selective inhibition of receptor-coupled phospholipase C-dependent processes in human platelets and polymorphonuclear neutrophils. *J. Pharmacol. Exp. Ther.* 255:756–768.

Boyer, J.L., I.E. Zohn, K.A. Jacobson, and T.K. Harden. 1994. Differential effects of P2-purinoceptor antagonists on phospholipase C- and adenylyl cyclase-coupled P2Y-purinoceptors. *Br. J. Pharmacol.* 113:614–620.

Bruzzone, S., L. Guida, E. Zocchi, L. Franco, and A. De Flora. 2001. Connexin 43 hemi channels mediate Ca2+-regulated transmembrane NAD+ fluxes in intact cells. *FASEB J.* 15:10–12.

Bruzzone, R., S.G. Hormuzdi, M.T. Barbe, A. Herb, and H. Monyer. 2003. Pannexins, a family of gap junction proteins expressed in brain. *Proc. Natl. Acad. Sci. USA*. 100:13644–13649. doi:10.1073/pnas.2233464100

Burnstock, G., and G.E. Knight. 2004. Cellular distribution and functions of P2 receptor subtypes in different systems. *Int. Rev. Cytol.* 240:31–304. doi:10.1016/S0074-7696(04)40002-3

Burnstock, G. 2007. Purine and pyrimidine receptors. *Cell. Mol. Life Sci.* 64:1471–1483. doi:10.1007/s00018-007-6497-0

Carpenter, C.L., and L.C. Cantley. 1996. Phosphoinositide kinases. *Curr. Opin. Cell Biol.* 8:153–158. doi:10.1016/S0955-0674(96)80060-3

Celetti, S.J., K.N. Cowan, S. Penuela, Q. Shao, J. Churko, and D.W. Laird. 2010. Implications of pannexin 1 and pannexin 3 for keratinocyte differentiation. *J. Cell Sci.* 123:1363–1372. doi:10.1242/jcs.056093

Chung, D.J., C.H. Castro, M. Watkins, J.P. Stains, M.Y. Chung, V.L. Szejnfeld, K. Willecke, M. Theis, and R. Civitelli. 2006. Low peak bone mass and attenuated anabolic response to parathyroid hormone in mice with an osteoblast-specific deletion of connexin43. *J. Cell Sci.* 119:4187–4198. doi:10.1242/jcs.03162

Civitelli, R., E.C. Beyer, P.M. Warlow, A.J. Robertson, S.T. Geist, and T.H. Steinberg. 1993. Connexin43 mediates direct intercellular communication in human osteoblastic cell networks. *J. Clin. Invest.* 91:1888–1896. doi:10.1172/JCI116406

Corriden, R., and P.A. Insel. 2010. Basal release of ATP: an autocrine-paracrine mechanism for cell regulation. *Sci. Signal.* 3:re1. doi:10.1126/scisignal.3104re1

D'hondt, C., R. Ponsaerts, H. De Smedt, G. Bultynck, and B. Himpens. 2009. Pannexins, distant relatives of the connexin family with specific cellular functions? *Bioessays*. 31:953–974. doi:10.1002/bies.200800236

Fill, M., and J.A. Copello. 2002. Ryanodine receptor calcium release channels. *Physiol. Rev.* 82:893–922.

Fujita, T., Y. Azuma, R. Fukuyama, Y. Hattori, C. Yoshida, M. Koida, K. Ogita, and T. Komori. 2004. Runx2 induces osteoblast and chondrocyte differentiation and enhances their migration by coupling with PI3K-Akt signaling. *J. Cell Biol.* 166:85–95. doi:10.1083/jcb.200401138

Futatsugi, A., T. Nakamura, M.K. Yamada, E. Ebisui, K. Nakamura, K. Uchida, T. Kitaguchi, H. Takahashi-Iwanaga, T. Noda, J. Aruga, and K. Mikoshiba. 2005. IP3 receptor types 2 and 3 mediate exocrine secretion underlying energy metabolism. *Science*. 309:2232–2234. doi:10.1126/science.1114110

Gramsch, B., H.D. Gabriel, M. Wiemann, R. Grümmer, E. Winterhager, D. Bingmann, and K. Schirrmacher. 2001. Enhancement of connexin 43 expression increases proliferation and differentiation of an osteoblast-like cell line. *Exp. Cell Res.* 264:397–407. doi:10.1006/excr.2000.5145

Grynkiewicz, G., M. Poenie, and R.Y. Tsien. 1985. A new generation of Ca2+ indicators with greatly improved fluorescence properties. *J. Biol. Chem.* 260:3440–3450.

Hoebertz, A., A. Townsend-Nicholson, R. Glass, G. Burnstock, and T.R. Arnett. 2000. Expression of P2 receptors in bone and cultured bone cells. *Bone*. 27:503–510. doi:10.1016/S8756-3282(00)00351-3

Inesi, G., and Y. Sagara. 1992. Thapsigargin, a high affinity and global inhibitor of intracellular Ca2+ transport ATPases. *Arch. Biochem. Biophys.* 298:313–317. doi:10.1016/0003-9861(92)90416-T

Inose, H., H. Ochi, A. Kimura, K. Fujita, R. Xu, S. Sato, M. Iwasaki, S. Sunamura, Y. Takeuchi, S. Fukumoto, et al. 2009. A microRNA regulatory mechanism of osteoblast differentiation. *Proc. Natl. Acad. Sci. USA*. 106:20794–20799. doi:10.1073/pnas.0909311106

Iwamoto, T., T. Nakamura, A. Doyle, M. Ishikawa, S. de Vega, S. Fukumoto, and Y. Yamada. 2010. Pannexin 3 regulates intracellular ATP/cAMP levels and promotes chondrocyte differentiation. *J. Biol. Chem.* 285:18948–18958. doi:10.1074/jbc.M110.127027

Jiang, J.X., A.J. Siller-Jackson, and S. Burra. 2007. Roles of gap junctions and hemichannels in bone cell functions and in signal transmission of mechanical stress. *Front. Biosci.* 12:1450–1462. doi:10.2741/2159

Kawamura, N., F. Kugimiya, Y. Oshima, S. Ohba, T. Ikeda, T. Saito, Y. Shinoda, Y. Kawasaki, N. Ogata, K. Hoshi, et al. 2007. Akt1 in osteoblasts and osteoclasts controls bone remodeling. *PLoS ONE*. 2:e1058. doi:10.1371/journal.pone.0001058

Ke, H.Z., H. Qi, A.F. Weidema, Q. Zhang, N. Panupinthu, D.T. Crawford, W.A. Grasser, V.M. Paralkar, M. Li, L.P. Audoly, et al. 2003. Deletion of the P2X7 nucleotide receptor reveals its regulatory roles in bone formation and resorption. *Mol. Endocrinol.* 17:1356–1367. doi:10.1210/me.2003-0021

Keller, D., and A.K. Grover. 2000. Nerve growth factor treatment alters Ca2+ pump levels in PC12 cells. *Neuroreport*. 11:65–68. doi:10.1097/00001756-200001170-00013

Koga, T., Y. Matsui, M. Asagiri, T. Kodama, B. de Crombrugghe, K. Nakashima, and H. Takayanagi. 2005. NFAT and Osterix cooperatively regulate bone formation. *Nat. Med.* 11:880–885. doi:10.1038/nm1270

Laird, D.W. 2006. Life cycle of connexins in health and disease. *Biochem. J.* 394:527–543. doi:10.1042/BJ20051922

Lecanda, F., P.M. Warlow, S. Sheikh, F. Furlan, T.H. Steinberg, and R. Civitelli. 2000. Connexin43 deficiency causes delayed ossification, craniofacial abnormalities, and osteoblast dysfunction. *J. Cell Biol.* 151:931–944. doi:10.1083/jcb.151.4.931

Lengner, C.J., H.A. Steinman, J. Gagnon, T.W. Smith, J.E. Henderson, B.E. Kream, G.S. Stein, J.B. Lian, and S.N. Jones. 2006. Osteoblast differentiation and skeletal development are regulated by Mdm2-p53 signaling. *J. Cell Biol.* 172:909–921. doi:10.1083/jcb.200508130

Li, J., D. Liu, H.Z. Ke, R.L. Duncan, and C.H. Turner. 2005. The P2X7 nucleotide receptor mediates skeletal mechanotransduction. *J. Biol. Chem.* 280:42952–42959. doi:10.1074/jbc.M506415200

Lian, J.B., G.S. Stein, A. Javed, A.J. van Wijnen, J.L. Stein, M. Montecino, M.Q. Hassan, T. Gaur, C.J. Lengner, and D.W. Young. 2006. Networks and hubs for the transcriptional control of osteoblastogenesis. *Rev. Endocr. Metab. Disord.* 7:1–16. doi:10.1007/s11154-006-9001-5

Maruyama, T., T. Kanaji, S. Nakade, T. Kanno, and K. Mikoshiba. 1997. 2APB, 2-aminoethoxydiphenyl borate, a membrane-penetrable modulator of Ins(1,4,5)P3-induced Ca2+ release. *J. Biochem.* 122:498–505.

Matsunobu, T., K. Torigoe, M. Ishikawa, S. de Vega, A.B. Kulkarni, Y. Iwamoto, and Y. Yamada. 2009. Critical roles of the TGF-beta type I receptor ALK5 in perichondrial formation and function, cartilage integrity, and osteoblast differentiation during growth plate development. *Dev. Biol.* 332:325–338. doi:10.1016/j.ydbio.2009.06.002

Mikoshiba, K. 2007. IP3 receptor/Ca2+ channel: from discovery to new signaling concepts. *J. Neurochem.* 102:1426–1446. doi:10.1111/j.1471-4159.2007.04825.x

Mukherjee, A., and P. Rotwein. 2009. Akt promotes BMP2-mediated osteoblast differentiation and bone development. *J. Cell Sci.* 122:716–726. doi:10.1242/jcs.042770

Nakashima, K., X. Zhou, G. Kunkel, Z. Zhang, J.M. Deng, R.R. Behringer, and B. de Crombrugghe. 2002. The novel zinc finger-containing transcription factor osterix is required for osteoblast differentiation and bone formation. *Cell.* 108:17–29. doi:10.1016/S0092-8674(01)00622-5

Ogawara, Y., S. Kishishita, T. Obata, Y. Isazawa, T. Suzuki, K. Tanaka, N. Masuyama, and Y. Gotoh. 2002. Akt enhances Mdm2-mediated ubiquitination and degradation of p53. *J. Biol. Chem.* 277:21843–21850. doi:10.1074/jbc.M109745200

Orriss, I.R., G.E. Knight, S. Ranasinghe, G. Burnstock, and T.R. Arnett. 2006. Osteoblast responses to nucleotides increase during differentiation. *Bone.* 39:300–309. doi:10.1016/j.bone.2006.02.063

Panchin, Y., I. Kelmanson, M. Matz, K. Lukyanov, N. Usman, and S. Lukyanov. 2000. A ubiquitous family of putative gap junction molecules. *Curr. Biol.* 10:R473–R474. doi:10.1016/S0960-9822(00)00576-5

Panupinthu, N., J.T. Rogers, L. Zhao, L.P. Solano-Flores, F. Possmayer, S.M. Sims, and S.J. Dixon. 2008. P2X7 receptors on osteoblasts couple to production of lysophosphatidic acid: a signaling axis promoting osteogenesis. *J. Cell Biol.* 181:859–871. doi:10.1083/jcb.200708037

Pardali, K., M. Kowanetz, C.H. Heldin, and A. Moustakas. 2005. Smad pathway-specific transcriptional regulation of the cell cycle inhibitor p21(WAF1/Cip1). *J. Cell. Physiol.* 204:260–272. doi:10.1002/jcp.20304

Penuela, S., R. Bhalla, X.Q. Gong, K.N. Cowan, S.J. Celetti, B.J. Cowan, D. Bai, Q. Shao, and D.W. Laird. 2007. Pannexin 1 and pannexin 3 are glycoproteins that exhibit many distinct characteristics from the connexin family of gap junction proteins. *J. Cell Sci.* 120:3772–3783. doi:10.1242/jcs.009514

Penuela, S., S.J. Celetti, R. Bhalla, Q. Shao, and D.W. Laird. 2008. Diverse subcellular distribution profiles of pannexin 1 and pannexin 3. *Cell Commun. Adhes.* 15:133–142. doi:10.1080/15419060802014115

Powell, J.A., M.A. Carrasco, D.S. Adams, B. Drouet, J. Rios, M. Müller, M. Estrada, and E. Jaimovich. 2001. IP(3) receptor function and localization in myotubes: an unexplored Ca(2+) signaling pathway in skeletal muscle. *J. Cell Sci.* 114:3673–3683.

Scemes, E., S.O. Suadicani, G. Dahl, and D.C. Spray. 2007. Connexin and pannexin mediated cell-cell communication. *Neuron Glia Biol.* 3:199–208. doi:10.1017/S1740925X08000069

Scherer, A., and J.M. Graff. 2000. Calmodulin differentially modulates Smad1 and Smad2 signaling. *J. Biol. Chem.* 275:41430–41438. doi:10.1074/jbc.M005727200

Seo, J.H., Y.H. Jin, H.M. Jeong, Y.J. Kim, H.G. Jeong, C.Y. Yeo, and K.Y. Lee. 2009. Calmodulin-dependent kinase II regulates Dlx5 during osteoblast differentiation. *Biochem. Biophys. Res. Commun.* 384:100–104. doi:10.1016/j.bbrc.2009.04.082

Solini, A., S. Cuccato, D. Ferrari, E. Santini, S. Gulinelli, M.G. Callegari, A. Dardano, P. Faviana, S. Madec, F. Di Virgilio, and F. Monzani. 2008. Increased P2X7 receptor expression and function in thyroid papillary cancer: a new potential marker of the disease? *Endocrinology.* 149:389–396. doi:10.1210/en.2007-1223

Stains, J.P., and R. Civitelli. 2005. Gap junctions in skeletal development and function. *Biochim. Biophys. Acta.* 1719:69–81. doi:10.1016/j.bbamem.2005.10.012

Su, M., J.L. Borke, H.J. Donahue, Z. Li, N.M. Warshawsky, C.M. Russell, and J.E. Lewis. 1997. Expression of connexin 43 in rat mandibular bone and periodontal ligament (PDL) cells during experimental tooth movement. *J. Dent. Res.* 76:1357–1366. doi:10.1177/00220345970760070501

Unger, V.M., N.M. Kumar, N.B. Gilula, and M. Yeager. 1999. Three-dimensional structure of a recombinant gap junction membrane channel. *Science.* 283:1176–1180. doi:10.1126/science.283.5405.1176

Vanden Abeele, F., G. Bidaux, D. Gordienko, B. Beck, Y.V. Panchin, A.V. Baranova, D.V. Ivanov, R. Skryma, and N. Prevarskaya. 2006. Functional implications of calcium permeability of the channel formed by pannexin 1. *J. Cell Biol.* 174:535–546. doi:10.1083/jcb.200601115

Vinken, M., T. Vanhaecke, P. Papeleu, S. Snykers, T. Henkens, and V. Rogiers. 2006. Connexins and their channels in cell growth and cell death. *Cell. Signal.* 18:592–600. doi:10.1016/j.cellsig.2005.08.012

Wang, X., H.Y. Kua, Y. Hu, K. Guo, Q. Zeng, Q. Wu, H.H. Ng, G. Karsenty, B. de Crombrugghe, J. Yeh, and B. Li. 2006. p53 functions as a negative regulator of osteoblastogenesis, osteoblast-dependent osteoclastogenesis, and bone remodeling. *J. Cell Biol.* 172:115–125. doi:10.1083/jcb.200507106

Wang, X.H., M. Streeter, Y.P. Liu, and H.B. Zhao. 2009. Identification and characterization of pannexin expression in the mammalian cochlea. *J. Comp. Neurol.* 512:336–346. doi:10.1002/cne.21898

Wicks, S.J., S. Lui, N. Abdel-Wahab, R.M. Mason, and A. Chantry. 2000. Inactivation of smad-transforming growth factor beta signaling by Ca(2+)-calmodulin-dependent protein kinase II. *Mol. Cell. Biol.* 20:8103–8111. doi:10.1128/MCB.20.21.8103-8111.2000

Zayzafoon, M. 2006. Calcium/calmodulin signaling controls osteoblast growth and differentiation. *J. Cell. Biochem.* 97:56–70. doi:10.1002/jcb.20675

Zayzafoon, M., K. Fulzele, and J.M. McDonald. 2005. Calmodulin and calmodulin-dependent kinase IIalpha regulate osteoblast differentiation by controlling c-fos expression. *J. Biol. Chem.* 280:7049–7059. doi:10.1074/jbc.M412680200

Ziganshin, A.U., C.H. Hoyle, G. Lambrecht, E. Mutschler, H.G. Bümert, and G. Burnstock. 1994. Selective antagonism by PPADS at P2X-purinoceptors in rabbit isolated blood vessels. *Br. J. Pharmacol.* 111:923–929.

THE JOURNAL OF BIOLOGICAL CHEMISTRY VOL. 287, NO. 13, pp. 10590–10601, March 23, 2012
Published in the U.S.A.

Role of Epithelial-Stem Cell Interactions during Dental Cell Differentiation*[S]

Received for publication, August 4, 2011, and in revised form, January 5, 2012 Published, JBC Papers in Press, February 1, 2012, DOI 10.1074/jbc.M111.285874

Makiko Arakaki[‡1], Masaki Ishikawa[§1], Takashi Nakamura[‡], Tsutomu Iwamoto[‡], Aya Yamada[‡], Emiko Fukumoto[‡], Masahiro Saito[¶], Keishi Otsu[‖], Hidemitsu Harada[‖], Yoshihiko Yamada[§], and Satoshi Fukumoto[‡2]

From the [‡]Division of Pediatric Dentistry, Department of Oral Health and Development Sciences, Tohoku University Graduate School of Dentistry, Sendai 980-8575, Japan, the [§]Laboratory of Cell and Developmental Biology, NIDCR, National Institutes of Health, Bethesda, Maryland 20892, the [¶]Faculty of Industrial Science and Technology, Tokyo University of Science, Chiba 278-8510, Japan, and the [‖]Department of Oral Anatomy II, Iwate Medical College School of Dentistry, Morioka 020-8505, Japan

Background: The role of dental epithelium in stem cell differentiation has not been clearly elucidated.
Results: SP cells differentiated into odontoblasts by epithelial BMP4, whereas iPS cells differentiated into ameloblasts when cultured with dental epithelium.
Conclusion: Stem cells can be induced to odontogenic cell fates when co-cultured with dental epithelium.
Significance: This is the first report to show induction of ameloblasts from iPS cells.

Epithelial-mesenchymal interactions regulate the growth and morphogenesis of ectodermal organs such as teeth. Dental pulp stem cells (DPSCs) are a part of dental mesenchyme, derived from the cranial neural crest, and differentiate into dentin forming odontoblasts. However, the interactions between DPSCs and epithelium have not been clearly elucidated. In this study, we established a mouse dental pulp stem cell line (SP) comprised of enriched side population cells that displayed a multipotent capacity to differentiate into odontogenic, osteogenic, adipogenic, and neurogenic cells. We also analyzed the interactions between SP cells and cells from the rat dental epithelial SF2 line. When cultured with SF2 cells, SP cells differentiated into odontoblasts that expressed dentin sialophosphoprotein. This differentiation was regulated by BMP2 and BMP4, and inhibited by the BMP antagonist Noggin. We also found that mouse iPS cells cultured with mitomycin C-treated SF2-24 cells displayed an epithelial cell-like morphology. Those cells expressed the epithelial cell markers p63 and cytokeratin-14, and the ameloblast markers ameloblastin and enamelin, whereas they did not express the endodermal cell marker Gata6 or mesodermal cell marker brachyury. This is the first report of differentiation of iPS cells into ameloblasts via interactions with dental epithelium. Co-culturing with dental epithelial cells appears to induce stem cell differentiation that favors an odontogenic cell fate, which may be a useful approach for tooth bioengineering strategies.

Tooth morphogenesis is characterized by reciprocal interactions between dental epithelium and mesenchymal cells derived from the cranial neural crest, which result in formation of the proper number and shapes of teeth. Multiple extracellular signaling molecules, including BMPs, FGFs, WNTs, and SHH, have been implicated in these interactions for tooth development (1). Epithelial cells then subsequently give rise to enamel-forming ameloblasts, while mesenchymal stem cells (MSCs)[3] form dentin-forming odontoblasts and dental pulp cells. Initial tooth development is also regulated by extracellular matrices (ECMs), such as basement membrane components that include laminin, collagen, fibronectin, and perlecan (2, 3). These matrices control proliferation, polarity, and attachment, and also determine tooth germ size and morphology. At later stages of tooth development, the basement membrane components disappear and odontogenic cells begin to secrete a variety of tooth-specific extracellular matrices that give rise to layers of enamel and dentin, produced by epithelial-derived ameloblasts and mesenchymal-derived odontoblasts, respectively. Ameloblastin (Ambn) is one of the enamel matrix proteins expressed by differentiating ameloblasts, and is essential for dental epithelial cell differentiation into ameloblasts and enamel formation (2, 4). Dentin sialophosphoprotein (DSPP) is a member of the SIBLING (Small Integrin-Binding Ligand *N*-linked Glycoprotein) family of extracellular matrix glycophosphoproteins, and is expressed by differentiating ameloblasts and odontoblasts (5). These extracellular matrices are important for the formation of enamel and dentin (2).

Stem cell research has identified and established several types of stem cells, including induced pluripotent stem (iPS) cells, which are generated from a variety of somatic cell types via introduction of transcription factors that mediate pluripo-

* This work was supported, in whole or in part, by the Intramural Research Program of the NIDCR, National Institutes of Health (to Y. Y.). This work was also supported by Grants-in-aid 20679006 (to S. F.), 21792054 (to A. Y.), 21792154 (to E. F.) from the Ministry of Education, Science, and Culture of Japan, and the NEXT program (LS010, to S. F.), and by grants from the Takeda Science Foundation.

[S] This article contains supplemental Figs. S1–S5 and Table S1.

[1] Both authors contributed equally to this work.
[2] To whom correspondence should be addressed: Division of Pediatric Dentistry, Department of Oral Health and Development Sciences, Tohoku University Graduate School of Dentistry, Sendai 980-8575, Japan. Fax: 81-22-717-8386; E-mail: fukumoto@dent.tohoku.ac.jp.

[3] The abbreviations used are: MSC, mesenchymal stem cell; mDP, mouse dental pulp; Ambn, Ameloblastin; DSPP, dentin sialophosphoprotein; iPS, induced pluripotent stem; DPSC, dental pulp stem cell; SP, side population; MP, majority population; ALP, alkaline phosphatase; MEF, mouse embryonic fibroblasts; MMC, mitomycin C.

tency (6). Direct reprogramming of somatic cells into iPS cells by forced expression of a small number of defined factors (*e.g.* Oct3/4, Sox2, Klf4, and c-Myc) has great potential for tissue-specific regenerative therapies. In addition, this process also avoids ethical issues surrounding the use of embryonic stem (ES) cells, as well as problems with rejection following implantation of non-autologous cells (7). A variety of cell types, including hematopoietic precursor cells (8, 9), endothelial cells, MSCs, neuronal cells (10), reproductive cells (11), and cardiomyocytes (12, 13), undergo *in vitro* differentiation. However previous studies of dental cell differentiation are not adequate to explain this process. Several dental stem cell populations have been identified in different parts of the tooth, including cells from the periodontal ligament that links the tooth root with the bone, tips of developing roots, and tissue (dental follicle) that surrounds an unerupted tooth. In addition, dental pulp stem cells (DPSCs) have been identified in the pulp of exfoliated deciduous teeth of both children and adults (14). These different cell types likely share a common lineage, being derived from neural crest cells, and all have generic MSC-like properties.

Transplantation of *in vitro* expanded DPSCs mixed with hydroxyapatite/tricalcium phosphate particles results in the formation of dental pulp and dentin-like tissue complexes in immunocompromised mice (15). Similar results have been observed with an MSC population obtained from human exfoliated deciduous teeth (SHED) (14). DPSCs also express the putative stem cell marker STRO-1 and perivascular cell marker CD146, while a proportion co-expresses smooth muscle actin and the pericyte-associated antigen 3G5 (16). These findings suggest that a population of DPSCs may reside in this perivascular niche within the pulp of adult teeth.

Side population (SP) cells were identified by flow cytometry analysis with a Hoechst 33342 efflux assay and found to have stem cell characteristics (17). SP cells are a small population that show low levels of Hoechst dye staining for the expression of Abcg2, an ATP-binding cassette transporter (18), which is strongly expressed in dental pulp in human adult and deciduous teeth (19). Dental pulp contains multipotent stem cells and is viewed as a potential source of iPS cells (14, 20, 21). In tooth germ development, undifferentiated neural crest-derived MSCs interact with dental epithelium and differentiate into dentin matrix-secreting odontoblasts. However, the interactions between stem cells and dental epithelium have not been clearly elucidated.

In this study, we established an SP cell line from mouse dental papilla. We then cultured these SP cells with rat dental epithelial cells to investigate epithelial-mesenchymal interactions. SP cells were induced to differentiate into DSPP expressing odontoblasts via the action of epithelial BMP4. Furthermore, mouse iPS cells differentiated into Ambn-expressing dental epithelium when cultured with dental epithelial cells. Thus, these undifferentiated stem cells can be induced to an odontogenic cell fate when co-cultured with dental epithelial cells. These findings may be useful for analysis of dental cell differentiation *in vitro* and for procurement of odontogenic cells for use in regenerative medicine.

EXPERIMENTAL PROCEDURES

Preparation of Mouse Dental Papilla Cells—Dental papilla tissues were isolated from incisors from newborn ICR mice by digesting with 0.1% collagenase D (Roche) and 2.5% trypsin for 30 min at 37 °C. Enzymatically digested tissues were minced into 2–4 mm pieces using micro-scissors and washed three times with Dulbecco's modified Eagle's medium (DMEM) (Invitrogen) containing 10% fetal bovine serum (FBS) (Invitrogen) and an antibiotic-antimycotic mixture (Invitrogen), then filtered through a cell strainer (40 μm) to eliminate clumps and debris. Mouse dental papilla (mDP) cells were cultured in 60-mm culture dishes and immortalized by expression of a mutant human papilloma virus type 16 E6 gene lacking the PDZ-domain-binding motif (22). mDP cells were maintained with DMEM supplemented with 10% FBS and an antibiotic-antimycotic mixture at 37 °C in a humidified atmosphere containing 5% CO_2.

Generation of Dental Epithelial Cell Line SF2-24 and Cell Culture—Rat dental epithelial cells were enzymatically isolated from the cervical loop at the apical end of the lower incisors from a Sprague-Dawley rat with 1% collagenase. Dental epithelial cells were cultured with DMEM (Invitrogen) supplemented with 10% FBS for 4 weeks, then, maintained in serum-free keratinocyte synthetic medium (Keratinocyte-SFM, Invitrogen) for 1 year. An established cell line, SF2 was maintained as previously described (4). SF2 cells were transfected with a pEF6/GFP-PDGFtm-myc-HA vector expressing the GFP-PDGF receptor-transmembrane fusion protein with myc-HA tag using Lipofectamine 2000 (Invitrogen). Transfected cells were selected as SF2 subclones by culturing with media containing 400 μg/ml of G418. Twenty-five clones were selected as a stable transfected cell line, with one of them designated as SF2-24 (Ambn high expression) and another SF2-7 (Ambn low expression).

SP and MP Cell Analysis and Flow Cytometry—Hoechst staining of mDP cells for SP cell analysis was conducted as previously described (17). Subconfluent mDP cells were stained with Hoechst dye for 90 min at 37 °C. After staining, all cells were resuspended in 100 μl of Hanks' balanced salt solution (HBSS) with calcium/magnesium medium and kept on ice. The SP and MP gates were defined as previously described (17). For analysis, the cells were resuspended in ice-cold HBSS with 2% FBS containing propidium iodide (Sigma) at a final concentration of 2 μg/ml to identify dead cells, then filtered through a cell strainer. Sorting and analyses were carried out with an EPICS ALTRA flow cytometer (Beckman Coulter, Fullerton, CA). The SP cell fraction was enriched by repeating cell sorting 3 times. The expression of stem cell markers in SP cells was confirmed by flow cytometry using anti-Sca-1 and Oct3/4 antibodies (Santa Cruz Biotechnology).

Differentiation of SP Cells—For odontoblastic induction, SP cells were plated at 6×10^4 cells in 60-mm dishes. After the cells had reached 50–60% confluence, we replaced the control medium with induction medium containing 100 ng/ml of BMP2 or BMP4 (Wako Pure Chemical Industries), and cells were incubated for 2 days. For blocking BMP signaling, recombinant mouse Noggin protein (R&D systems) was

used. Total RNA was isolated and real time RT-PCR was performed using mouse Bcrp1 (18) and DSPP primer sets (supplemental Table S1).

For adipogenic differentiation, SP cells were seeded at 1×10^5 cells per well in 6-well plates and cultured in DMEM supplemented with 10% FBS. Adipogenic differentiation was induced with induction medium from a Poietics hMSC Media Bullet kit (Cambrex Bio Science Walkersville, Inc., Walkersville, MD) for 3 days and incubated in maintenance medium for 3 days, then the cells were cultured for an additional 7 days in maintenance medium. As a control, cells were cultured in only maintenance medium. Adipogenesis was confirmed by staining with Oil-Red-O and the expression of *PPARγ* was analyzed by RT-PCR.

For osteogenic differentiation, SP cells were seeded at 1.5×10^4 cells per well in 6-well plates and cultured in DMEM supplemented with 10% FBS, 10 mM β-glycerophosphate, 0.2 mM ascorbic acid, 2-phosphate, and 10^{-8} M dexamethasone. Induction and control media were replaced every 2 days. Osteogenesis was determined by alkaline phosphatase (ALP) and von Kossa staining for calcium deposition, as previously described (23). After 4 weeks culturing with osteoblast induction medium, the expressions of osteocalcin, osteonectin, and Runx2 in osteogenesis-induced SP cells were analyzed by RT-PCR.

For neurogenic differentiation, we modified a neuronal induction protocol using recombinant nerve growth factor (NGF) (Chemicon). SP cells were seeded at 1×10^5 cells per well in 6-well plates. After reaching 80–90% confluence, neurogenic differentiation was induced by culturing the cells in DMEM supplemented 2% FBS, 1.25% dimethyl sulfoxide, 10^{-6} M retinoic acid, 2.5 μg/ml insulin, and 50 ng/ml NGF. Two weeks later, neurogenesis was characterized by Western blot analysis using an anti-neurofilament-M specific antibody (Cell Signaling Technology).

Odontoblastic Induction of SP Cells by Co-culturing with Dental Epithelial Cells—We investigated the role of dental epithelial cells in specification of odontogenic cell lineage using two types of co-culture systems: feeder and chamber types with a cell culture insert (BD Falcon). We used confluent SF2 cells, or SF2 cells treated with 4% paraformaldehyde (PFA) or ammonium (denudation) as feeder cells. SF2 and SP cells were harvested and placed into either 6-well plates or cell culture inserts (chamber), then cultured until reaching confluence.

Screening of Co-culture Conditions for Ameloblastic Induction of iPS Cells—A mouse iPS cell line (iPS-MEF-Ng-20D-17), carrying the Nanog-GFP/IRES/puromycin resistant gene, was established by Yamanaka (Kyoto University, Japan), and obtained from RIKEN Cell Bank (Saitama, Japan) (6). Mouse iPS cells were cultured with rat dental epithelial cells (SF2-24), which predominantly express Ambn mRNA, as feeder cells. Preparatory co-culture experiments were performed as follows: iPS cells were cultured with mouse embryonic fibroblasts (MEFs) treated with mitomycin C (MMC) or with three different types of SF2-24 feeder cells (confluent cells, cells treated with MMC, cells treated with 4% PFA). MMC was supplied at 9 μg/ml (final concentration) for 2 h to arrest SF2-24 cell proliferation.

Induction of iPS Cell-derived Ameloblasts—iPS cells (plated $1.5 \times 10^3/cm^2$) were cultured on sheets of MMC-treated SF2-24 cells for 7, 10, and 14 days in the same medium used for the SF2-24 culture without leukemia inhibitory factor and 2-mercaptoethanol. The culture medium was changed every day throughout the co-culture period. After 7 and 10 days, the co-cultured iPS cells were subjected to RT-PCR, while those after 14 days of culture were analyzed by immunocytochemistry. Total RNA from iPS cells co-cultured with MMC-treated MEFs was isolated after 3 days of culture. Conditioned media from cultures of SF2-24 and SF2-7 were collected after 2 days of incubation. The procedures used for transfection of Ambn-expressing vectors, as well as their construction and isolation of recombinant proteins have been previously described (2, 24). K252a (Trk inhibitor, Calbiochem), PD98059 (MEK inhibitor, Cell signaling), anti-NT-4 neutralizing antibody (Applied Biological Materials), and Noggin (R&D systems) were added to conditioned medium obtained from SF2-24 cells.

Reverse Transcription-PCR—Total RNA was isolated using TRIzol (Invitrogen) and first-strand cDNA was synthesized at 50 °C for 50 min using oligo(dT) or random primers with the SuperScript III First-strand Synthesis System (Invitrogen). PCR was performed with Takara Ex Taq HotStart Version (Takara) or a PCR Additives Kit (Jena Bioscience, Germany). The primer sequences are presented in supplemental Table S1. PCR amplicons were separated and visualized on 1.5% agarose gels with SYBR Green staining using the LAS-4000 mini image analyzing system (Fujifilm). For semi-quantitative PCR analysis, the band intensities of PCR amplicons were quantified using MultiGauge software (Fujifilm) and normalized by dividing the intensity of the band of GAPDH. Because of the high degree of homology between the Ambn gene in mice and rats (94.2%), we designed a species-specific mouse Ambn primer that encoded locked nucleic acid (LNA) at a different base sequence between the mouse and rat Ambn gene in a conserved region. The specificity of the mouse Ambn primer was confirmed by PCR using mouse and rat tooth germ cDNA. Statistical analysis of gene expression was performed using the Student's *t* test.

Immunocytochemistry—For immunocytochemistry, cells were fixed with 4% PFA for 5 min at room temperature. After washing with PBS three times for 5 min, the cells were treated with Power Block Universal Reagent (BioGenex) for 5 min at room temperature, followed by three washes with PBS. The cells were incubated with the anti-Ambn primary antibody included in the kit (1:200, M-300, Santa Cruz Biotechnology). The primary antibody was visualized with Alexa Fluor 594 donkey anti-rabbit antibody (1:500, A21207, Invitrogen). Nuclei were stained with Hoechst 33258 (Invitrogen). Immunocytochemistry and phase images were captured using a BZ-8000 microscopic system (KEYENCE Co, Osaka, Japan), and images of the sections were analyzed using a BZ analyzer (KEYENCE).

RESULTS

Establishment of SP Cell Line from Mouse Dental Papilla Cells—Side population (SP) cells, which displayed stem cell ability, make up less than 1% of total cells in the mouse dental papilla (mDP) from postnatal tooth germs. Thus, biochemical and biomolecular analyses of SP cells are difficult to perform

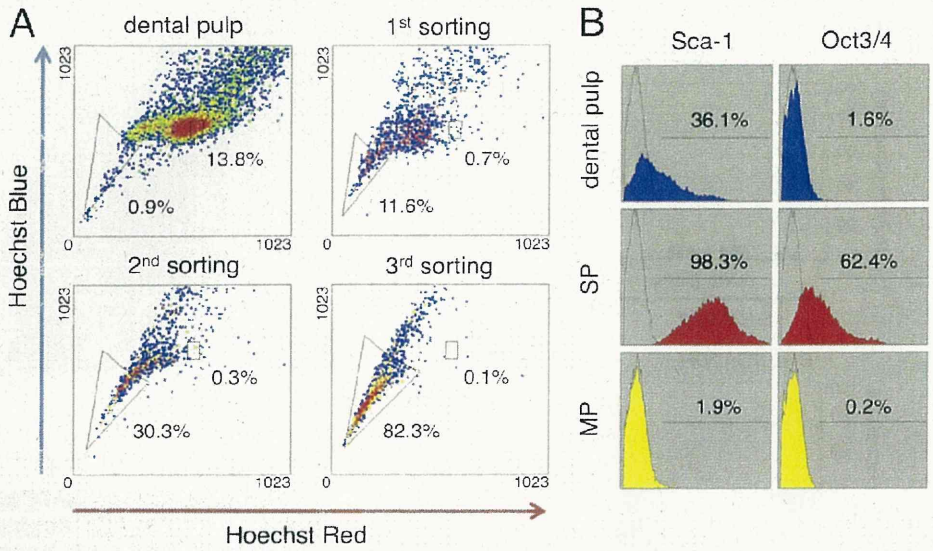

FIGURE 1. **Isolation of SP cells from mDP cell line.** *A*, flow cytometry analysis of SP cells. mDP cells made up ~0.9% of the total cell population with a relatively lower level of Hoechst 33342 fluorescence (SP cells), while 13.8% of the population was maintained as MP cells. Using repeated cell sorting, the SP cell population was enriched by 11.6% at the first sorting, 30.3% at the second sorting, and 82.3% at the third sorting. *B*, expression of the stem cell markers Sca-1 and Oct3/4 in dental pulp, SP, and MP cells.

because of the limited numbers of cells available. We enriched an SP cell population and established an SP cell line using a cell sorting technique. mDP cells were obtained from mouse incisor tooth germs and immortalized, as previously described (22). The cells were then stained with Hoechst dye and sorted to enrich the SP cell fraction. Cell sorting was repeated three times and SP cells were enriched from about 0.9% to 82.3% in the gated area (Fig. 1*A*). This SP cell line showed high expression levels of the stem cell markers Sca-1 and Oct3/4 when compared with the majority population (MP) cells, which was comprised of a greater number dental papilla cells in various differentiation stages (Fig. 1*B*).

Because the SP cells expressed a set of stem cell markers, we examined their multipotency. Using an odontoblast differentiation medium containing BMP2 or BMP4, the SP cells were induced to express DSPP, a marker of odontoblasts, whereas the expression of the undifferentiated cell marker Bcrp1 was decreased (Fig. 2*A*). In osteoblast differentiation medium, the SP cells showed increased levels of ALP and von Kossa staining, as well as expressions of the osteoblast marker genes osteocalcin, osteonectin, and Runx2, whereas the MP cells showed no induction of expression of those genes (Fig. 2, *B* and *C*). When SP cells were cultured in differentiation medium for adipogenesis or neurogenesis, they were Oil-Red-O positive or showed neurite outgrowths, along with high levels of adipogenic expression and protein expressions of neurogenic markers, such as *PPARγ* and Neurofilament-M, respectively (supplemental Fig. S1, *A*–*D*). These results suggest that the SP cell line established in this study has a high level of multipotency.

Expressions of Runx2 and DSPP in SP Cells Cultured with SF2 Cells—We analyzed epithelial and mesenchymal stem cell interactions by culturing SP cells with rat dental epithelial SF2 cells that had been engineered to express a GFP-myc-HA tag on the cell membrane surface. This allowed us to distinguish between SP and SF2 cell types (supplemental Fig. S2). SP cells were cultured with or without SF2 cells for 48 h, and total RNA was isolated from the mixed cell cultures (Fig. 3*A*). The expressions of Runx2 and DSPP were increased in SP cells that had been cultured with SF2 cells, as compared with those cultured without SF2 cells (Fig. 3*B*). Because Runx2 and DSPP are expressed by both odontoblasts and ameloblasts, co-cultured SP and SF2 cells were separated into individual cell populations using the anti-HA antibody, which specifically recognizes SF2 cells (Fig. 3*C*). We found a dramatic increase in the expression level of Runx2 in SF2 cells as compared with SP cells (Fig. 3*D*). No epithelial marker was detected in SP cells co-cultured with SF2 cells, suggesting that the SP cells had differentiated into odontoblasts (data not shown). Runx2 is expressed in enamel matrix-secreting ameloblasts, but not in the pre-secretion stage of ameloblasts (25). Our results suggest that the SF2 cells had fully differentiated into enamel matrix-secreting ameloblasts by co-culturing with SP cells. The expression of DSPP was up-regulated in both cell types. However, in MP cells, which are fully differentiated dental papilla cells, no expression of Runx2 or DSPP was induced by co-culturing with SF2 cells (data not shown). These results indicate that epithelial and mesenchymal stem cell interactions promote individual differential states in SF2 and SP cells.

Involvement of Exogenous Factors from Dental Epithelium in DSPP Expression of SP Cells—We attempted to identify the factors in dental epithelial cells involved in SP cell differentiation by treating SF2 cells with 4% PFA to inhibit extracellular signaling, including the effects of growth factors (Fig. 4*A*). Ammonia treatment, through a process known as denudation, removes all cell components except the extracellular matrices and is often used for three-dimensional matrix cell culture experiments (26). DSPP expression in SP cells was partially inhibited by PFA treatment, while they retained the extracellular matrix network. This result suggests that the extracellular environment including extracellular matrices, growth factors, and cell-cell

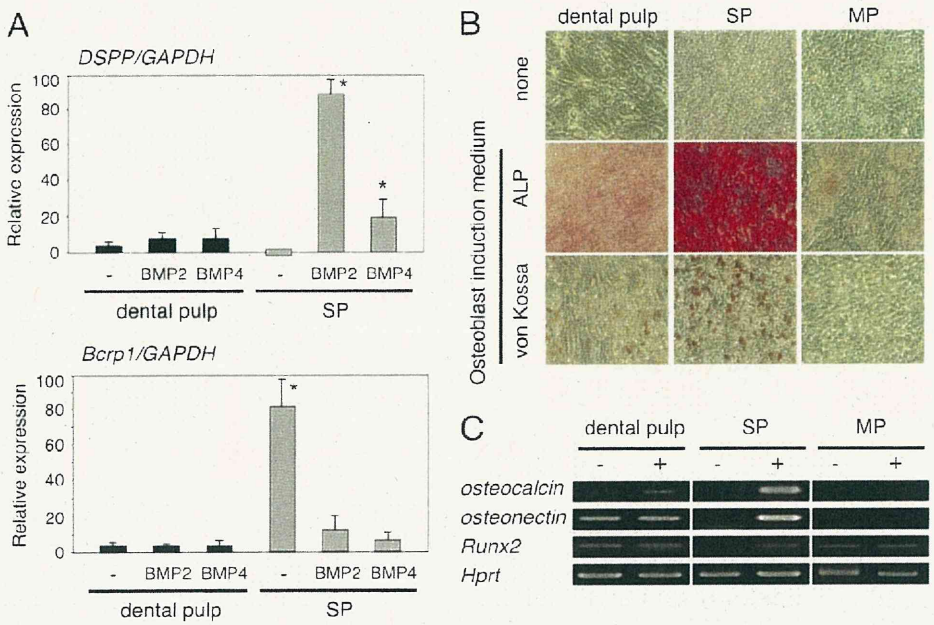

FIGURE 2. **Odontoblast and osteoblast differentiation in SP cells.** *A*, differentiation of SP cells to odontoblasts. Expression of the odontoblast marker DSPP and the undifferentiated mesenchymal marker Bcrp1 in dental pulp (*black bar*) and SP cells (*gray bar*) cultured with or without BMP2 or BMP4. *B*, differentiation of SP cells to osteoblasts in osteoblast induction medium (*Osteogenic cond.*). ALP and von Kossa staining of dental pulp, SP, and MP cells. *C*, expressions of osteoblast markers in dental pulp, SP, and MP cells cultured in regular (−) or osteoblast induction medium (+). *, $p < 0.05$.

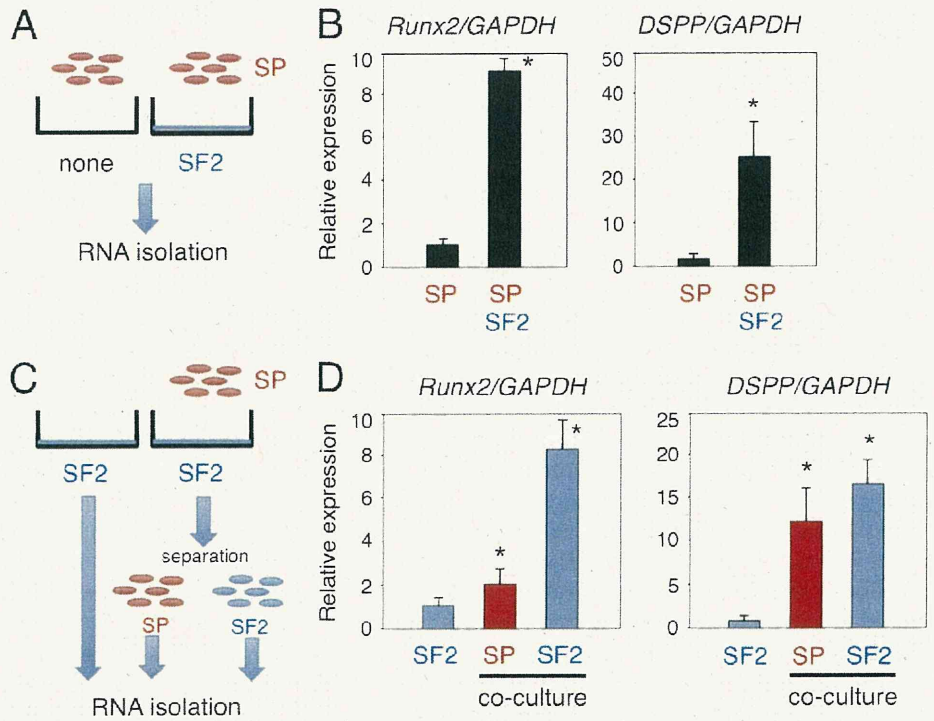

FIGURE 3. ***In vitro* epithelial-mesenchymal interaction system using dental epithelial cells (*SF2*) and dental mesenchymal stem cells (*SP*) to promote odontogenic cell differentiation.** *A* and *C*, schematic diagram of the co-culture system. *B*, comparisons of *Runx2* and *DSPP* gene expressions between the SP monolayer culture and SP and SF2 cell co-culture system. *C*, total RNA samples were separately prepared from SP and SF2 cells, using the anti-HA antibody. *D*, expressions of Runx2 and DSPP in co-cultured SF2 (*blue*) and SP (*red*) cells. The expression level of GAPDH was used an internal control. *, $p < 0.05$.

interaction produced by SF2 cells contributes to odontoblast induction. Denuded SF2 cells were also incapable of inducing DSPP expression in SP cells (Fig. 4*B*). Odontoblast induction of SP cells was observed in co-cultures with living SF2 cells, indicating that some types of soluble secreted molecules and matrices from SF2 cells are required to induce SP cells to undergo odontogenic differentiation.

Next, we screened the factors secreted from SF2 cells that promote odontogenic cell differentiation from epithelial and mesenchymal cells using cell culture chambers, which allowed

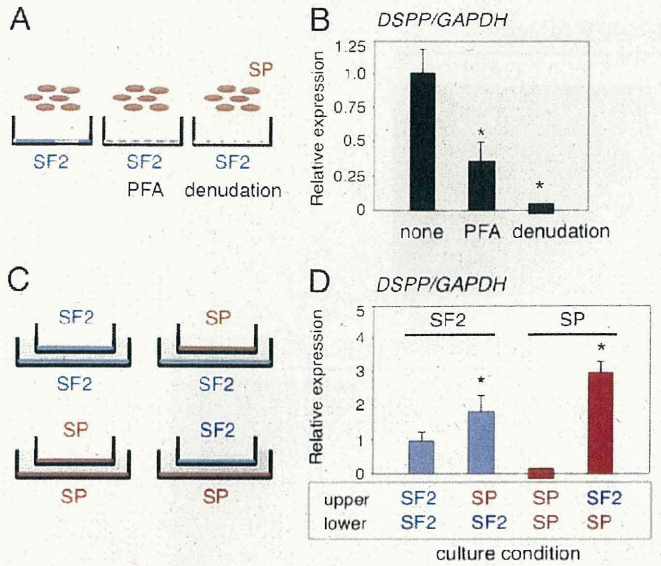

FIGURE 4. **Co-culture conditions for screening of odontogenic cell differentiation using *in vitro* cell-cell interaction system.** *A*, SP cells were cultured on SF2 cells in monolayers, then fixed with 4% paraformaldehyde (*PFA*) or treated with ammonia (denudation). *B*, DSPP expression in SP cells co-cultured under different conditions. *C*, four sets of co-culture conditions using cell chambers were analyzed. *D*, DSPP expression in SF2 cells (*blue*) and SP cells (*red*) cultured in lower dishes, with co-culture partner cells in the upper chambers. The expression level of GAPDH was used an internal control. *, $p < 0.05$.

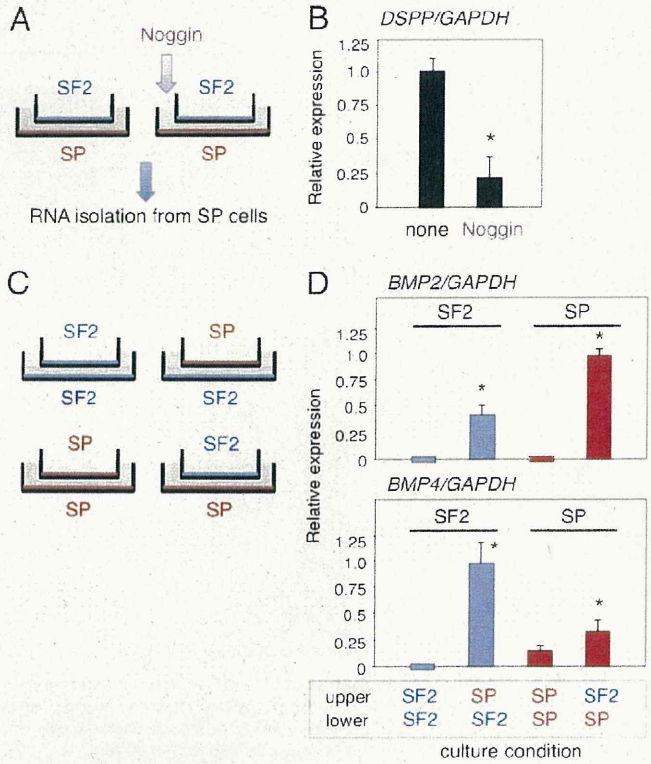

FIGURE 5. ***In vitro* epithelial-mesenchymal interaction system shows that crosstalk BMP signaling is essential for odontogenic cell differentiation.** *A*, total RNA was isolated from SP cells co-cultured with SF2 cells in the presence or absence of Noggin recombinant protein. *B*, DSPP expression in SP cells co-cultured with SF2 cells after blocking BMP signaling. *C*, four sets of culture conditions using cell chambers were analyzed. *D*, BMP2 and BMP4 expressions in SF2 (*blue*) and SP (*red*) cells, with co-culture partner cells in the upper chambers. *, $p < 0.05$.

the factors to be secreted into cell culture medium (Fig. 4*C*). Heterologous combinations of SF2 and SP cells were important for promotion of DSPP expression in both types of cells. We found that co-cultures consisting of SF2 cells in the upper chamber and SP cells in the lower chamber were most effective for stimulation of DSPP gene expression in SP cells (Fig. 4*D*). These results suggest that secreted factors are important for induction of DSPP expression in SP cells co-cultured with dental epithelial cells.

Regulation of DSPP Expression in SP Cells via BMP2-BMP4 Crosstalk—The involvement of several different types of growth factors has been reported in epithelial-mesenchymal interactions, for example, BMPs were shown to promote dental mesenchymal cell differentiation (27). We examined the potential involvement of BMPs in SP cell differentiation by adding soluble Noggin, which antagonizes BMP activity, to cell chamber cultures that contained SP cells in the lower chambers (Fig. 5*A*). The presence of Noggin in culture medium resulted in down-regulation of the expression of DSPP in SP cells as compared with the control cells (Fig. 5*B*). Therefore, BMPs are required for induction of DSPP expression in SP cells co-cultured with dental epithelial cells. In tooth germ development, BMP4 is involved in epithelial-mesenchymal interaction, and also regulates the mesenchymal expression of Msx1 and Msx2, which are important for tooth development, whereas BMP2 promotes dental mesenchymal differentiation (27). However, details regarding crosstalk between BMP2 and BMP4 in dental epithelial and mesenchymal stem cell interactions have not been elucidated. We sought to clarify the role of BMPs in these interactions by examining the expressions of BMP2 and BMP4 in SF2 and SP cells using a separated chamber assay (Fig. 5*C*). The expression of BMP2 was higher in SP cells than SF2 cells under the heterologous combination culture condition, whereas BMP2 was not detected in homologous cultures (Fig. 5*D*). In contrast, the expression of BMP4 was higher in SF2 cells than in SP cells in the heterologous combinations (Fig. 5*D*). Taken together, these results suggest that the interactions between dental epithelium and dental mesenchymal stem cells induce BMP4 and BMP2, which, in turn, promote odontogenic cell differentiation via paracrine and autocrine signaling.

Optimization of Co-culture Conditions for Differentiation of iPS Cells into Ambn-expressing Dental Epithelial Cells—Following interaction with SF2 cells, SP cells differentiated into DSPP expressing cells, but not ameloblasts (Figs. 3, 4, and 5). This may be because SP cells are mesenchymal stem cells and committed to differentiate into mesenchyme lineage cell types. Therefore, we used mouse iPS cells to examine whether these cells can be differentiated into ameloblasts when cultured with SF2 cells. However, SF2 cells did not effectively promote their differentiation (data not shown), which may be due to the necessity of factors from differentiated dental epithelial cells for differentiation of iPS cells into ameloblasts. To test this possibility, we subcloned 25 different SF2 cell lines and examined the expression levels of the Ambn gene. Of these lines, the SF2-24 cell line expressed Ambn at the highest level (supplemental Fig. S3*A*). Dental epithelium SF2-24 cells grew tightly together in a

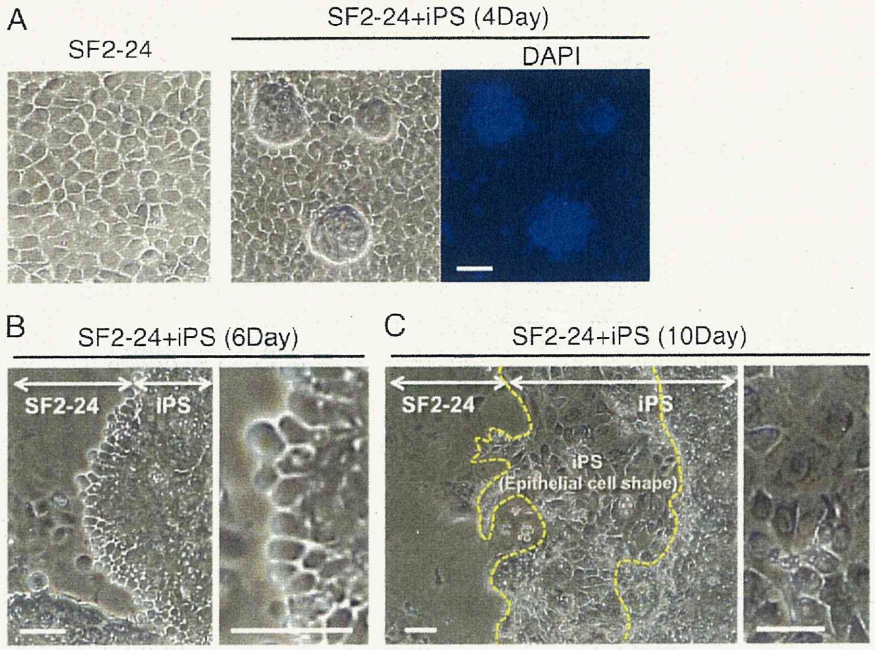

FIGURE 6. **Epithelial cell shapes of iPS cells after co-culturing with SF2-24 cells.** *A*, phase micrographs of monolayer SF2-24 cells and iPS cells cultured with SF2-24 feeder cells for 4 days, followed by DAPI staining. *B* and *C*, low and high magnification phase micrographs of iPS cells on MMC-treated SF2-24 feeder cells after 6 (*6Day*) and 10 days (*10Day*). Enlarged image shows a part of the iPS cells with epithelial cell shapes. *C*, epithelial cell cluster formed by iPS cell-derived epithelial cells (area within *yellow dashed line*). Bar, 50 mm.

square or cuboidal shape (Fig. 6*A*), and expressed Ambn and cytokeratin-14 (CK14), but not the reprogrammed factors Sox2, Klf4, and Oct3/4 (supplemental Fig. S3*B*). On the other hand, iPS cells formed colonies that expressed Nanog promoter-driven GFP (data not shown) as well as Klf4, Sox2, Oct3/4, and Nanog, but not Ambn or CK14 (supplemental Fig. S3*B*).

We also examined the effects of differentiation by co-culturing iPS cells with MMC-treated non-proliferating SF2-24 feeder cells (Fig. 6*A*). The shape of the co-cultured iPS cells was clearly rounded along the boundary of the clusters after 6 days (Fig. 6*B*). These cells had migrated and formed what appeared to be epithelium after 10 days (area surrounded by *yellow dashed line*, Fig. 6*C*).

The differentiation of iPS cells was then determined by RT-PCR analysis. First, we examined the specificity of mouse Ambn locked nucleic acid (LNA) primer sets (supplemental Fig. S4). A mouse Ambn LNA primer set specifically detected the mouse Ambn gene, but not the rat Ambn gene (supplemental Fig. S4*A*). Using this primer set, Ambn expression was not detected in mouse iPS cells or MEFs (supplemental Fig. S4*B*). Next, we examined co-culture conditions for the differentiation of iPS cells into dental epithelium (Fig. 7*A*). iPS cells co-cultured with MMC-treated SF2-24 cells showed a high expression of the mouse Ambn gene, while those co-cultured with PFA-treated or non-treated SF2-24 cells did not (Fig. 7*B*). SF2-24 feeder cells expressed rat Ambn when co-cultured with iPS cells, while that expression was reduced at 10 days (Fig. 7*C*).

Interestingly, expressions of the stem cell markers Sox2, Oct3/4, Nanog, Fgf4, and Gdf3 were not changed throughout the co-culture period, because of the existence of undifferentiated iPS cells (Fig. 7*C*), while those of the endodermal markers Cdx2 and Gata6 were also not increased. Furthermore, the mesodermal marker Brachyury was highly expressed in iPS cells, because of technical contamination resulting RNA extraction from MEFs used for maintenance of the iPS cells, and then gradually decreased over time. We also observed increased expressions of the mouse ameloblast markers Ambn and Enamelin (Enam), as well as the epithelial markers CK14 and p63, in iPS cells after 7 and 10 days (Fig. 7*C*). Furthermore, the expression of epiprofin/Sp6, a transcription factor highly expressed in dental epithelium (28), was increased in those cells (supplemental Fig. S5). A similar expression pattern was observed in co-cultured iPS cells separated from SF2-24 cells using the anti-HA antibody (data not shown).

Differentiation of iPS Cells into Ambn-expressing Dental Epithelial Cells—We then examined the protein expression of Ambn in iPS cells using immunostaining. Approximately 95% of the epithelial-like cells were positive for Ambn (Fig. 8*A*), while the immunofluorescence intensity of Ambn was stronger in iPS cells than in SF2-24 cells (Fig. 8*B*). Therefore, mouse iPS cells differentiated into dental epithelium, but not into endodermal or mesodermal cells.

We attempted to identify the factors involved in differentiation of iPS cells into dental epithelium by culturing with MEFs in medium conditioned by SF2-24 cell cultures (Fig. 9*A*). Culturing with SF2-24 condition medium induced the expression of Ambn in iPS cells, indicating an involvement of soluble factors including growth factors, and extracellular matrices derived from SF2-24 cells (Fig. 9*B*). Next, we examined the effect of Ambn on differentiation of iPS cells into dental epithelial cells. Expression vectors for the full-length (AB1), C-terminal (AB2), and N-terminal (AB3) half of Ambn (Fig. 9*C*) were separately transfected into Ambn low-expressing cells (SF2-7), then conditioned media from those cells or recombinant Ambn

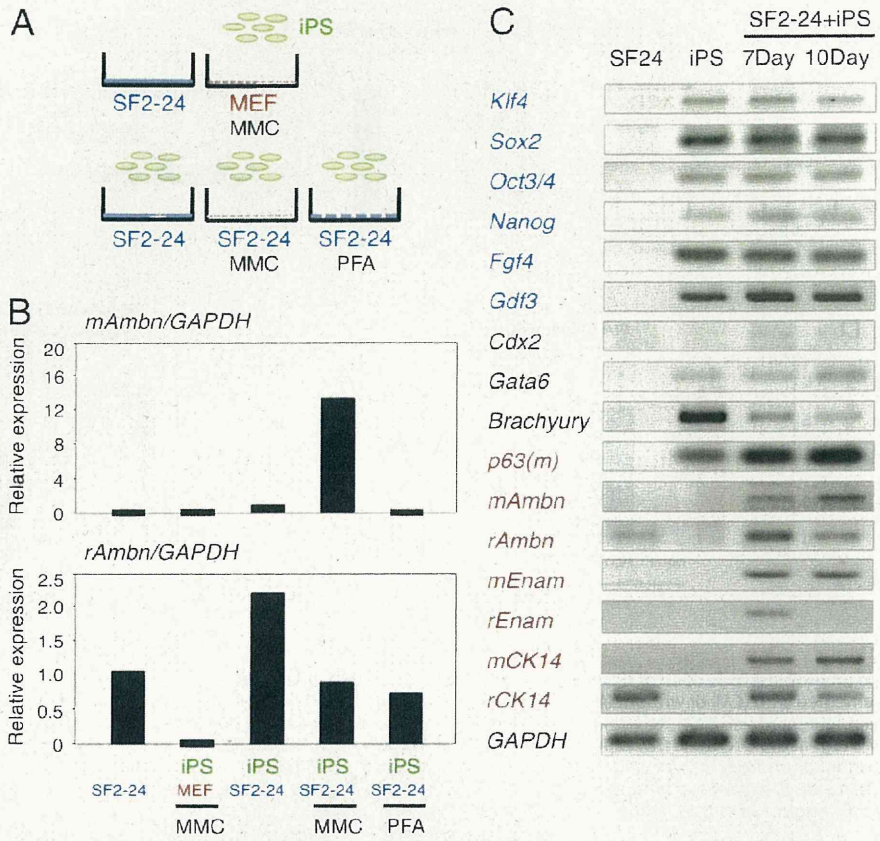

FIGURE 7. **Effects of culture conditions on ameloblast induction of iPS cells.** *A*, iPS cells were co-cultured with SF2-24 cells, MMC-treated (*MMC*) MEFs, MMC-treated SF2-24 cells or PFA-treated SF2-24 cells. *B*, Ambn expression in mouse iPS (*upper panel*) and rat-derived SF2-24 (*bottom panel*) cells in different co-culture conditions for 10 days. *C*, time course analysis of gene expressions of stem cell (*blue*), endo/mesoderm (*black*), and ameloblast (*red*) markers in iPS cells co-cultured with SF2-24 cells for 7 (*7Day*) and 10 days (*10Day*).

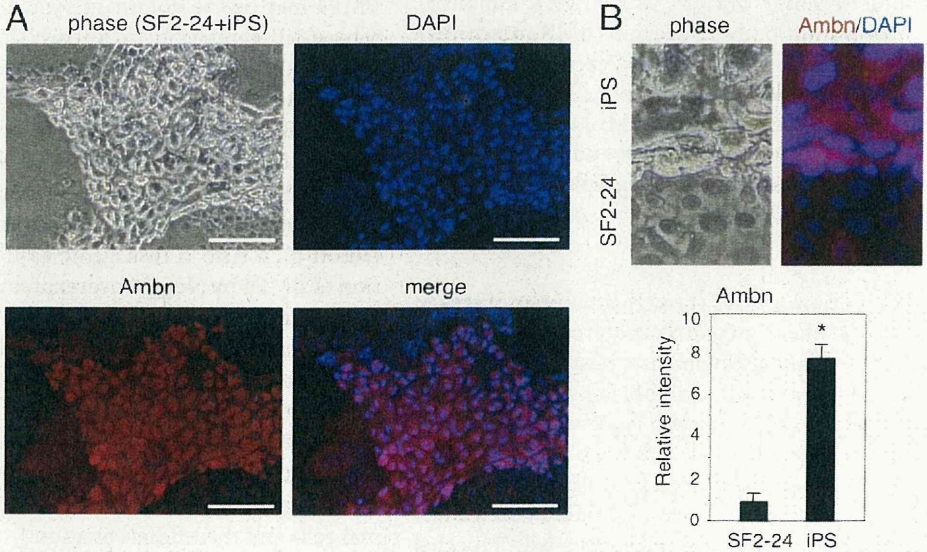

FIGURE 8. **Expression of Ambn, an ameloblast specific protein, in iPS cells co-cultured with SF2-24 cells.** *A*, phase micrographs of iPS cell colonies cultured with mitomycin C-treated SF2-24 cells. Hoechst staining (*blue*), Ambn staining (*red*), and merged images. *B*, high magnifications of phase and merged images in *A*. *Bottom panel*, relative expression levels of Ambn protein in SF2-24 and iPS cells cultured in ameloblast induction system. *, $p < 0.05$; Bar, 100 mm.

proteins (AB1, -2, or -3) were added to cultures of iPS cells. Conditioned media from SF2-24 cells and full-length AMBN-expressing cells, but not from other transfectants or recombinant Ambn proteins, induced Ambn expression in iPS cells (Fig. 9*D*), indicating that Ambn may be necessary for differentiation of iPS cells into dental epithelium. Previously, we showed that neurotrophic factor NT-4 is important for the differentiation of ameloblasts (29). To examine the effect of NT-4

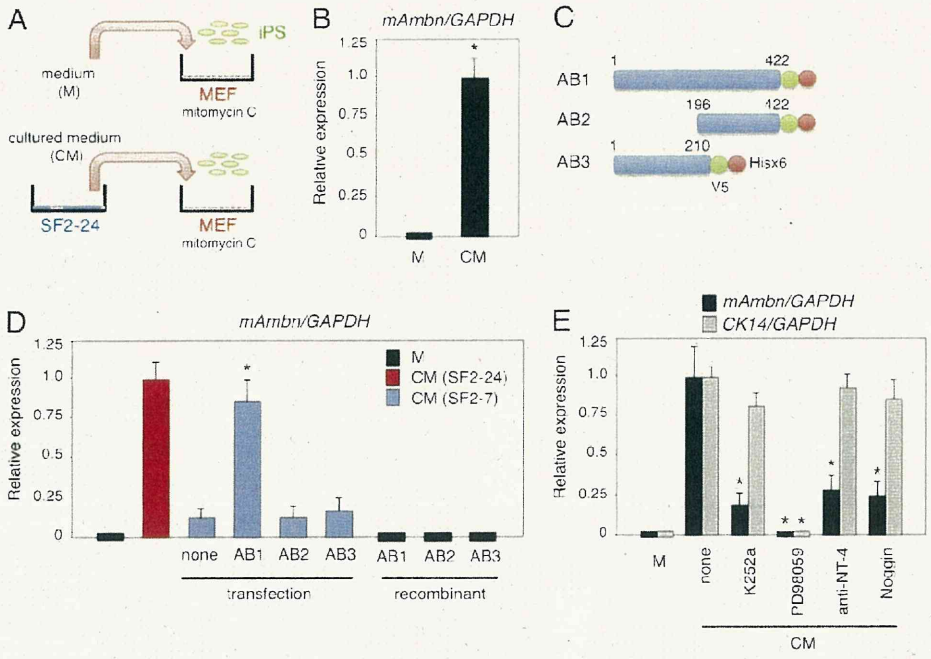

FIGURE 9. **Promotion of ameloblast induction of iPS cells using conditioned SF2-24 cells.** *A*, iPS cells were cultured on mitomycin C-treated MEFs in iPS cell culture medium supplemented with (*CM*) or without (*M*) conditioned medium from SF2-24 cells. *B*, expression of mouse Ambn gene in iPS cells cultured in iPS cell culture medium supplemented with (*CM*) or without (*M*) conditioned medium from SF2-24 cells. *C*, creation of Ambn deletions. All recombinant Ambn proteins have V5 and His tags at the C terminus. *D*, expression of mouse Ambn gene in iPS cells cultured in iPS cell culture medium supplemented with (*CM*) or without (*M*) condition medium from SF2-24 cells, recombinant Ambn-expressing SF2-7 cells or recombinant Ambn proteins. *, $p < 0.05$ (compared with non-transfected SF2-7 cells). *E*, expression of mouse Ambn and CK14 genes in iPS cells cultured in SF2-24 conditioned medium supplemented with K252a, PD98059, anti-NT-4, or Noggin. *, $p < 0.05$ (compared with CM only).

on dental epithelial cell differentiation by iPS cells, we analyzed the expressions of Ambn and CK14 in iPS cells cultured with SF2-24-conditioned medium in the presence of K252a (inhibitor of neurotrophic receptor Trk), PD98059 (MEK inhibitor), anti-NT-4 neutralizing antibody, or Noggin (BMP antagonist). K252a, PD98059, anti-NT-4, and Noggin each inhibited the expression of Ambn in iPS cells. Furthermore, CK14 expression in iPS cells was not inhibited by K252a, anti-NT-4, or Noggin (Fig. 9*E*). These results indicate that NT-4 and BMP signaling are important for differentiation into dental epithelial cells, but not CK14-positive epithelial cells.

DISCUSSION

Tooth development progresses through a number of stages, and the differentiation of dentin matrix-secreting odontoblasts and enamel matrix-producing ameloblasts results in formation of the crown. Ameloblasts and odontoblasts are central cell types involved in tooth development. In developing molars, restricted dental mesenchymal cells interact with the inner dental epithelium through the matrix and differentiate into odontoblasts. In the present study, we established an SP cell line from dental papilla mDP cells using cell sorting with Hoechst staining. SP cells are known to retain multipotency characteristics and can differentiate into various cell types, such as odontoblasts, osteoblasts, adipocytes, and neural cells. Our method for obtaining multipotent SP cells from a single cell line may be useful for development of novel therapeutic strategies that aim at regeneration of oral tissues.

Our co-culture assay of SP cells with dental epithelial cells showed that dental epithelial cells promote SP cell differentiation into DSPP-expressing cells via BMP2 and BMP4, which are secreted from dental epithelial cells (Fig. 5*B*, 5*D*, and 10*A*). Because BMP2 is not highly expressed in dental epithelium, BMP4 may be the dominant signaling regulator during odontoblast differentiation. In the early stages of tooth development, BMP4 is expressed in dental epithelium and induces the transcription factor Msx1 (30). The expression of DSPP is induced via the BMP signaling pathway in cooperation with Runx2, Dlx5, and Msx1 in undifferentiated mesenchymal cells (31). Previously, a bead soak assay of mandibular organ culture showed that BMP4 induced dental mesenchymal cell differentiation (32). Also, a transgenic approach revealed that inhibition of BMP4 by Noggin overexpression, driven by a keratin 14 promoter (K14-Noggin), resulted in the absence of all molars in the mandible. This indicates that BMP4 is essential for tooth bud formation by inducing dental mesenchymal cells (33). As demonstrated, in the present study odontoblastic differentiation of SP cells is completely disturbed by the blocking of BMP signaling. Thus, our finding strongly support the notion that BMP4 signaling is a key factor in induction of dental mesenchymal cells and their differentiation.

Differential synchronization between dental epithelial and mesenchymal cells has been observed during tooth development. Dental epithelial and mesenchymal cells are separated by a basement membrane, which is an essential regulator for epithelial-mesenchymal interaction (34). Both crown and root odontoblasts are induced by interactions with epithelial cells, such as those of the inner dental epithelium, epithelial rest, and epithelial diaphragm (35). Similar to *in vivo* situations, physical

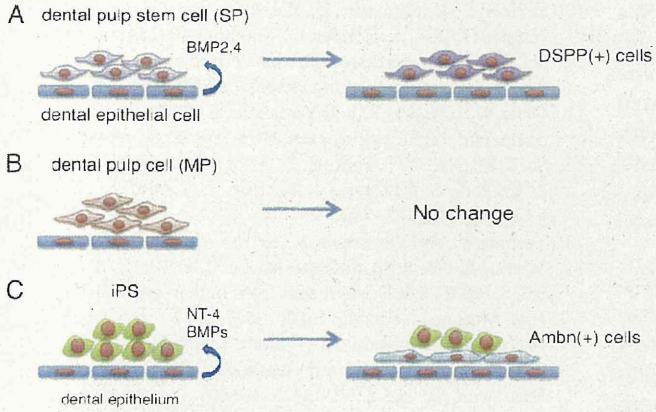

FIGURE 10. **Proposed models of odontogenic induction from dental mesenchymal stem cells and iPS cells by co-culturing with dental epithelial cells.** *A*, dental epithelial cells induce DSPP-expressing odontoblasts from SP cells. *B*, no odontogenic induction was observed in differentiated (*MP*) cells co-cultured with dental epithelial cells. *C*, dental epithelial cells induce Ambn-expressing ameloblasts from iPS cells.

cell attachment of dental epithelial cells was not required for odontogenic induction of SP cells in our experiments, indicating that soluble factors including BMPs are important for odontogenic induction by dental epithelial cells in culture. We also found that MP cells from dental papilla did not differentiate into DSPP-expressing cells, indicating that epithelial-mesenchymal interactions are important for cell fate determination of dental pulp stem cells, but not for differentiated dental pulp cells (Fig. 10, *A* and *B*). It was recently reported that Ambn protein, or a synthetic peptide based on the N-terminal region of the Ambn protein, induced osteoblastic cell differentiation (36). In addition to BMPs, Ambn may also be one of the factors involved in the odontogenic induction process, because the sharing of signaling pathways underlies the mechanism of odontoblastic and osteoblastic induction.

Ameloblasts secrete enamel-specific extracellular matrices including Ambn, which are lost upon tooth eruption. This makes it impossible to repair or replace damaged enamel in an erupted tooth. Therefore, identifying alternative sources of these cells becomes important. Bone marrow-derived cells can give rise to different types of epithelial cells. In mixed cultures with c-Kit+-enriched bone marrow cells, embryonic dental epithelial cells, and dental mesenchyme, bone marrow cells might be reprogrammed to give rise to ameloblast-like cells (37). Our strategy to create ameloblasts from mouse iPS cells may have direct application in tooth regeneration. We succeeded in establishing a co-culture system using cells derived from two different species, mouse iPS cells and rat derived enamel matrix secreting ameloblasts. This is the first demonstration of differentiation of iPS cells into ameloblasts through interactions with dental epithelium (Fig. 10*C*). However, a set of stem cell markers was continuously expressed in iPS cells after 7 days of co-culturing (Fig. 7*C*), indicating that a portion of the iPS cells had differentiated into enamel-secreting ameloblasts and some still retained stem cell potential. Thus, the efficacy of iPS cell differentiation into ameloblasts by enamel-secreting ameloblasts feeder cells must to be improved prior to for clinical application.

A number of factors are thought to give iPS cells the capacity for direct or indirect differentiation into ameloblasts. Possible direct effectors include gap junctions, intercellular binding molecules, adhesion factors, and extracellular matrices secreted by dental epithelium. Growth factors might also be involved, because conditioned medium from SF2-24 cells induced Ambn expression in iPS cells. Ambn is also a candidate factor for dental cell differentiation of iPS cells, as SF2 cells expressing low levels of Ambn did not induce differentiation of iPS cells. Furthermore, overexpression of full-length Ambn in cells expressing low levels of Ambn induced iPS cells into ameloblast-like differentiation (Fig. 9*D*). Ambn has diverse functions in various cellular physiologies, such as cell growth, differentiation, cell polarization, and attachment, though the detailed mechanisms of Ambn signaling require additional investigation. Ambn-null mice display severe enamel hypoplasia due to impaired dental epithelial cell proliferation, polarization, and differentiation into ameloblasts, as well as loss of cell attachment activity with immature enamel matrix (2). These results suggest that Ambn, especially full-length, is necessary for both *in vivo* and *in vitro* ameloblast differentiation.

There were differences in cell lineage determination of the dental pulp stem cells and iPS cells when co-cultured with dental epithelial cells. RT-PCR analysis showed that co-culturing induced SP cells to form odontoblastic cells, whereas iPS cells were induced to form ameloblastic cells. In addition, the expression of Brachyury, a mesodermal marker, in iPS cells was down-regulated by co-culturing with SF2-24 cells (Fig. 7*C*). Conversely, expressions of the epithelial markers p63 and CK14, as well as the dental epithelial marker epiprofin/Sp6 were up-regulated (Fig. 7*C*, supplemental Fig. S5) (28). These results suggest that the cell lineage of the iPS cells in our co-culturing system was effectively guided into an epithelial cell lineage. It has been reported that the default cell lineage of ES cells is the ectodermal cells, except when cultured in the presence of BMP antagonists (38, 39). Because BMPs promote ectodermal differentiation of ES cells, the expression of BMP observed in SF2 cells (Fig. 5*D*) may also contribute to dental epithelial cell differentiation of iPS cells. A previous our reported that NT-4 induced Ambn expression in dental epithelium, while NT-4 knock-out mice showed delayed expression of enamel matrices in the early stage of ameloblast differentiation (29). In the present study, the presence of the anti-NT-4 neutralizing antibody or Noggin in conditioned medium from SF2-24 cells inhibited Ambn expression, but not that of CK14 (Fig. 9*E*). On the other hand, SP cells strongly expressed the endogenous Sox2 protein, one of the reprogramming factors involved in generation of iPS cells (data not shown). Recently, iPS cells were generated from human dental pulp cells with a high level of efficiency in comparison to dermal fibroblasts, possibly due to a high expression level of Sox2 in dental pulp stem cells. However, additional reprogramming factors are required for creation of iPS cells from dental pulp cells. Thus, SP cells themselves did not have the same degree of multipotency as seen with ES and iPS cells. SP cells are considered to be mesenchymal stem cells that originate from dental pulp cells, which are derived from cranial neural crest cells. Neural crest cells can differentiate into several different cell lineages, such as neuron, glia, melanocyte,

osteoblast, chondrocyte, and odontoblast cells (40, 41). We believe that SP cells are not able to gain multipotency beyond the potential of neural crest cells. Thus, SP cells preserve some degree of multipotency that is different in an undifferentiated state as compared with ES and iPS cells. In co-cultures with SF2-24 cells, SP cells did not differentiate into ameloblasts, whereas iPS cells did (Fig. 10). Comparative analysis between SP and iPS cells is essential to clarify the mechanisms involved in directional cell fate determination.

In this study, we sought to clarify the role of dental epithelium and stem cell interactions by culturing rat dental epithelium with mouse iPS cells and SP cells. Rodent incisors grow throughout the lifespan of the animal by maintaining stem cells in the cervical loop, located at the end of incisor. A dental epithelial cell niche also exists in the cervical loop of the incisor. Analysis of gene knock-out mice for epiprofin/Sp6, an essential transcription factor for dental epithelial cell differentiation and enamel formation, has revealed that supernumerary teeth are formed by interactions between dental mesenchyme and undifferentiated dental epithelium (4, 42). In addition, those studies showed continuous signals from dental epithelial cells of mutant mice induced the continued differentiation of dental mesenchymal cells into odontoblasts (4, 42). Together these findings suggest that dental epithelial cells can induce dental mesenchymal cells to differentiate into odontoblasts. Therefore, rat dental epithelial cells may provide an *in vitro* niche environment for surrounding mouse iPS cells and SP cells. Elucidation of the mechanism of cell fate determination by dental epithelial cells may facilitate development of novel therapeutic approaches for regenerative dentistry.

REFERENCES

1. Thesleff, I. (2003) Epithelial-mesenchymal signaling regulating tooth morphogenesis. *J. Cell Sci.* **116,** 1647–1648
2. Fukumoto, S., Kiba, T., Hall, B., Iehara, N., Nakamura, T., Longenecker, G., Krebsbach, P. H., Nanci, A., Kulkarni, A. B., and Yamada, Y. (2004) Ameloblastin is a cell adhesion molecule required for maintaining the differentiation state of ameloblasts. *J. Cell Biol.* **167,** 973–983
3. Yuasa, K., Fukumoto, S., Kamasaki, Y., Yamada, A., Fukumoto, E., Kanaoka, K., Saito, K., Harada, H., Arikawa-Hirasawa, E., Miyagoe-Suzuki, Y., Takeda, S., Okamoto, K., Kato, Y., and Fujiwara, T. (2004) Laminin $\alpha 2$ is essential for odontoblast differentiation regulating dentin sialoprotein expression. *J. Biol. Chem.* **279,** 10286–10292
4. Nakamura, T., de Vega, S., Fukumoto, S., Jimenez, L., Unda, F., and Yamada, Y. (2008) Transcription factor epiprofin is essential for tooth morphogenesis by regulating epithelial cell fate and tooth number. *J. Biol. Chem.* **283,** 4825–4833
5. Fisher, L. W., and Fedarko, N. S. (2003) Six genes expressed in bones and teeth encode the current members of the SIBLING family of proteins. *Connect Tissue Res.* **44,** Suppl. 1, 33–40
6. Takahashi, K., Tanabe, K., Ohnuki, M., Narita, M., Ichisaka, T., Tomoda, K., and Yamanaka, S. (2007) Induction of pluripotent stem cells from adult human fibroblasts by defined factors. *Cell* **131,** 861–872
7. Lewitzky, M., and Yamanaka, S. (2007) Reprogramming somatic cells towards pluripotency by defined factors. *Curr. Opin. Biotechnol.* **18,** 467–473
8. Xu, D., Alipio, Z., Fink, L. M., Adcock, D. M., Yang, J., Ward, D. C., and Ma, Y. (2009) Phenotypic correction of murine hemophilia A using an iPS cell-based therapy. *Proc. Natl. Acad. Sci. U.S.A.* **106,** 808–813
9. Hanna, J., Wernig, M., Markoulaki, S., Sun, C. W., Meissner, A., Cassady, J. P., Beard, C., Brambrink, T., Wu, L. C., Townes, T. M., and Jaenisch, R. (2007) Treatment of sickle cell anemia mouse model with iPS cells generated from autologous skin. *Science* **318,** 1920–1923
10. Soldner, F., Hockemeyer, D., Beard, C., Gao, Q., Bell, G. W., Cook, E. G., Hargus, G., Blak, A., Cooper, O., Mitalipova, M., Isacson, O., and Jaenisch, R. (2009) Parkinson disease patient-derived induced pluripotent stem cells free of viral reprogramming factors. *Cell* **136,** 964–977
11. Okita, K., Ichisaka, T., and Yamanaka, S. (2007) Generation of germline-competent induced pluripotent stem cells. *Nature* **448,** 313–317
12. So, K. H., Han, Y. J., Park, H. Y., Kim, J. G., Sung, D. J., Bae, Y. M., Yang, B. C., Park, S. B., Chang, S. K., Kim, E. Y., and Park, S. P. (2010) *Int. J. Cardiol.* **153,** 277–285
13. Yoshida, Y., and Yamanaka, S. (2011) *J. Mol. Cell Cardiol.* **50,** 327–332
14. Miura, M., Gronthos, S., Zhao, M., Lu, B., Fisher, L. W., Robey, P. G., and Shi, S. (2003) SHED: stem cells from human exfoliated deciduous teeth. *Proc. Natl. Acad. Sci. U.S.A.* **100,** 5807–5812
15. Gronthos, S., Mankani, M., Brahim, J., Robey, P. G., and Shi, S. (2000) Postnatal human dental pulp stem cells (DPSCs) *in vitro* and *in vivo*. *Proc. Natl. Acad. Sci. U.S.A.* **97,** 13625–13630
16. Shi, S., Bartold, P. M., Miura, M., Seo, B. M., Robey, P. G., and Gronthos, S. (2005) The efficacy of mesenchymal stem cells to regenerate and repair dental structures. *Orthod. Craniofac Res.* **8,** 191–199
17. Goodell, M. A., Brose, K., Paradis, G., Conner, A. S., and Mulligan, R. C. (1996) Isolation and functional properties of murine hematopoietic stem cells that are replicating *in vivo*. *J. Exp. Med.* **183,** 1797–1806
18. Zhou, S., Schuetz, J. D., Bunting, K. D., Colapietro, A. M., Sampath, J., Morris, J. J., Lagutina, I., Grosveld, G. C., Osawa, M., Nakauchi, H., and Sorrentino, B. P. (2001) The ABC transporter Bcrp1/ABCG2 is expressed in a wide variety of stem cells and is a molecular determinant of the side-population phenotype. *Nat. Med.* **7,** 1028–1034
19. Li, L., Kwon, H. J., Harada, H., Ohshima, H., Cho, S. W., and Jung, H. S. (2011) Expression patterns of ABCG2, Bmi-1, Oct-3/4, and Yap in the developing mouse incisor. *Gene Expr. Patterns* **11,** 163–170
20. Nam, H., and Lee, G. (2009) Identification of novel epithelial stem cell-like cells in human deciduous dental pulp. *Biochem. Biophys. Res. Commun.* **386,** 135–139
21. Yan, X., Qin, H., Qu, C., Tuan, R. S., Shi, S., and Huang, G. T. (2010) iPS cells reprogrammed from human mesenchymal-like stem/progenitor cells of dental tissue origin. *Stem. Cells Dev.* **19,** 469–480
22. Yokoi, T., Saito, M., Kiyono, T., Iseki, S., Kosaka, K., Nishida, E., Tsubakimoto, T., Harada, H., Eto, K., Noguchi, T., and Teranaka, T. (2007) Establishment of immortalized dental follicle cells for generating periodontal ligament *in vivo*. *Cell Tissue Res.* **327,** 301–311
23. Klotz, O. (1905) Studies upon calcareous degeneration: I. The process of pathological calcification. *J. Exp. Med.* **7,** 633–674
24. Sonoda, A., Iwamoto, T., Nakamura, T., Fukumoto, E., Yoshizaki, K., Yamada, A., Arakaki, M., Harada, H., Nonaka, K., Nakamura, S., Yamada, Y., and Fukumoto, S. (2009) Critical role of heparin binding domains of ameloblastin for dental epithelium cell adhesion and ameloblastoma proliferation. *J. Biol. Chem.* **284,** 27176–27184
25. Chen, S., Gu, T. T., Sreenath, T., Kulkarni, A. B., Karsenty, G., and MacDougall, M. (2002) Spatial expression of Cbfa1/Runx2 isoforms in teeth and characterization of binding sites in the *DSPP* gene. *Connect. Tissue Res.* **43,** 338–344
26. Cukierman, E., Pankov, R., Stevens, D. R., and Yamada, K. M. (2001) Taking cell-matrix adhesions to the third dimension. *Science* **294,** 1708–1712
27. Nakashima, M. (1994) Induction of dentin formation on canine amputated pulp by recombinant human bone morphogenetic proteins (BMP)-2 and -4. *J. Dent. Res.* **73,** 1515–1522
28. Nakamura, T., Unda, F., de-Vega, S., Vilaxa, A., Fukumoto, S., Yamada, K. M., and Yamada, Y. (2004) The Krüppel-like factor epiprofin is expressed by epithelium of developing teeth, hair follicles, and limb buds and promotes cell proliferation. *J. Biol. Chem.* **279,** 626–634
29. Yoshizaki, K., Yamamoto, S., Yamada, A., Yuasa, K., Iwamoto, T., Fukumoto, E., Harada, H., Saito, M., Nakasima, A., Nonaka, K., Yamada, Y., and Fukumoto, S. (2008) Neurotrophic factor neurotrophin-4 regulates ameloblastin expression via full-length TrkB. *J. Biol. Chem.* **283,** 3385–3391
30. Chen, Y., Bei, M., Woo, I., Satokata, I., and Maas, R. (1996) Msx1 controls inductive signaling in mammalian tooth morphogenesis. *Development* **122,** 3035–3044

31. Cho, Y. D., Yoon, W. J., Woo, K. M., Baek, J. H., Park, J. C., and Ryoo, H. M. (2010) The canonical BMP signaling pathway plays a crucial part in stimulation of dentin sialophosphoprotein expression by BMP-2. *J. Biol. Chem.* **285,** 36369–36376
32. Vainio, S., Karavanova, I., Jowett, A., and Thesleff, I. (1993) Identification of BMP-4 as a signal mediating secondary induction between epithelial and mesenchymal tissues during early tooth development. *Cell* **75,** 45–58
33. Plikus, M. V., Zeichner-David, M., Mayer, J. A., Reyna, J., Bringas, P., Thewissen, J. G., Snead, M. L., Chai, Y., and Chuong, C. M. (2005) Morphoregulation of teeth: modulating the number, size, shape and differentiation by tuning Bmp activity. *Evol. Dev.* **7,** 440–457
34. Thesleff, I., and Hurmerinta, K. (1981) Tissue interactions in tooth development. *Differentiation* **18,** 75–88
35. Ten Cate, A. R. (1996) The role of epithelium in the development, structure and function of the tissues of tooth support. *Oral Dis.* **2,** 55–62
36. Iizuka, S., Kudo, Y., Yoshida, M., Tsunematsu, T., Yoshiko, Y., Uchida, T., Ogawa, I., Miyauchi, M., and Takata, T. (2011) Ameloblastin regulates osteogenic differentiation by inhibiting Src kinase via cross talk between integrin β1 and CD63. *Mol. Cell Biol.* **31,** 783–792
37. Hu, B., Unda, F., Bopp-Kuchler, S., Jimenez, L., Wang, X. J., Haïkel, Y., Wang, S. L., and Lesot, H. (2006) Bone marrow cells can give rise to ameloblast-like cells. *J. Dent. Res.* **85,** 416–421
38. Chang, C., and Hemmati-Brivanlou, A. (1998) Cell fate determination in embryonic ectoderm. *J. Neurobiol.* **36,** 128–151
39. Muñoz-Sanjuan, I., and Brivanlou, A. H. (2002) Neural induction, the default model and embryonic stem cells. *Nat. Rev. Neurosci.* **3,** 271–280
40. Baroffio, A., Dupin, E., and Le Douarin, N. M. (1991) Common precursors for neural and mesectodermal derivatives in the cephalic neural crest. *Development* **112,** 301–305
41. Sieber-Blum, M., and Cohen, A. M. (1980) Clonal analysis of quail neural crest cells: they are pluripotent and differentiate *in vitro* in the absence of noncrest cells. *Dev. Biol.* **80,** 96–106
42. Nakamura, T., Fukumoto, S., and Yamada, Y. (2011) Review: diverse function of epiprofin in tooth development. *J. Oral Biosci.* **53,** 22–30

Glycosphingolipids Regulate Ameloblastin Expression in Dental Epithelial Cells

Y. Kamasaki, T. Nakamura, K. Yoshizaki, T. Iwamoto, A. Yamada, E. Fukumoto, Y. Maruya, K. Iwabuchi, K. Furukawa, T Fujiwara and S. Fukumoto

J DENT RES 2012 91: 78 originally published online 6 October 2011

DOI: 10.1177/0022034511424408